Fractionation in a dike in the Tuolumne Batholith in California

Rhobeca Oliveros

Advisors: Dr. Philip Piccoli and Dr. Richard Ash

Geol 394

Fall 2017

Abstract

Fractionation is a process by which the mineral composition is differentiated across the area of an igneous body. The focus of this study is a dike that crops out on Lembert Dome in the Tuolumne Intrusive Complex (TIC). The TIC displays concentric compositional and textural zoning that has been interpreted to be the result of fractionation. The dike crops out near the interior, youngest component of the TIC in the Cathedral Peak region, and represents one of the last portions of the melt in the region to crystallize. Based on the timing of crystallization, which is late relative to the rest of the intrusive complex, I expect to see higher concentrations of rare earth and trace elements as compared to the country rock. I also expect to see fractionation along the length of the dike. I used optical microscopy, Electron Probe Micro-analysis, and Laser Ablation Inductively Coupled Plasma Mass Spectrometry to characterize the chemical composition of the minerals in various locations on the dike and to measure the relative concentrations of rare earth and trace elements in the constituent minerals. I was able to interpret the role fractionation played in the dikes formation by measuring the variation in chemical composition in biotite, plagioclase feldspar, and potassium feldspar. From analyses completed using EPMA and LA-ICP-MS, I found variation in the chemistry, mineralogy, and texture of the minerals as it relates to the location in the dike, which I conclude are results of fractionation.

Introduction

Fractionation occurs in igneous bodies due to differentiation in the melt as the magma cools. This is because different minerals crystallize at different pressures and temperatures; as the system cools, minerals precipitate, changing the composition of the remaining melt as cooling progresses. I used three primary methods to examine the chemical composition of minerals in a dike that crops out on Lembert Dome in Yosemite National Park: optical microscopy, Electron Probe Micro-analysis (EPMA) and Laser Ablation Inductively Coupled Plasma Mass Spectrometry (LA-ICP-MS).

A dike is an igneous intrusion that propagates through preexisting rocks. The dike that is the focus of this study is in the Tuolumne Intrusive Complex (TIC) and it may represent some of the latest stages of crystallization of the whole intrusive complex. The basis of this study is to characterize the mineralogy and analyze the chemistry of the minerals in the surrounding country rock and at different points within the dike, from which I found a measureable correlation between the location and the chemical and mineralogical characteristics. Chemistry of minerals from samples along the dike were determined using EPMA and with that, mineral formulas were calculated. LA-ICP-MS yielded concentrations of rare earth and trace elements in the minerals that were examined with EPMA.

The TIC is an advantageous location to study fractionation in dikes and concentrations of rare earth and trace elements for a number of reasons. First, the exposure and polish of the surfaces have made the underlying features of the rock easily accessible. Not only does this give insight into the features of the rock, it makes it much easier to collect samples. Next, Yosemite

National Park was first protected by legislation in 1890, so it has remained mostly intact without significant changes brought on by development or industry. Finally, it has been a very popular place to study for over a century, so there is an abundance of literature and previous studies to reference for my research.

Hypothesis

My hypothesis is that there will be a variation in the chemistry of the major elements in the major rock-forming minerals of the dike (biotite, potassium feldspar, and plagioclase feldspar), as well as in the concentrations of the rare earth and trace elements related to the location along the length of the dike, as a result of fractionation.

My null hypothesis is that there is no correlation between the chemistry and composition of the minerals and the location within the dike.

Geologic Background

The dike crops out on Lembert Dome in the Tuolumne Meadows area of the TIC, part of the larger Sierra Nevada Batholith. Most of the batholith is located in Yosemite National Park in California. Its' formation is associated with the Sevier Orogeny of western North America. The rocks that comprise the TIC formed 88.1 ± 0.2 million years ago. The TIC as a whole formed between 93 million years ago to 85 million years ago during the Late Cretaceous, dates that were calculated using U-Pb dating methods (Coleman et al., 2004). The TIC has a rough "peanut" shape, with the narrowest section being approximately 10 km across and 60 km long. It is one of four or five (depending on the source cited) that collectively comprise the Sierra Nevada Batholith. There is huge variation of textures and compositions across the TIC, which is believed to be due to fractionation as it formed (Bateman and Chappell, 1979). The rock types range from granodiorites to granites and the textures range from phaneritic to equigranular to porphyritic from the outermost portions of the batholith to the center (Paterson et al., 2011). The dike is an aplitic granodiorite, located in the Cathedral Peak region of the TIC, and is approximately 2 m wide at the widest section and about 180 m long. A photograph of the distal end of the dike can be found below; additional photographs of the dike can be found in appendix 1 and a schematic in appendix 4.

Figure 1. The distal end of the dike and the surrounding Cathedral Peak country rock, lens cap for scale. Photo by Philip Piccoli.

Similar to the way the TIC as a whole is fractionated, the dike shows evidence of fractionation and represents one of the last portions of the melt in this complex to crystallize. The exact age of the dike is not measured nor will it be part of this study, but it is younger than Lembert Dome on the basis of cross cutting relationships. There are two mechanisms that could have driven this fractionation: “preferential accretion of crystalline material present in the magma to the margins of the magma chamber… and/or downward settling of crystals, probably accompanied by upward movement of melt and volatiles” (Bateman and Chappell, 1979). The diagram below illustrates the direction that fractionation will take in a dike. The fine grained outer zones of an igneous body may be an effect of liquidus undercooling, whereas the coarse texture of the interior zones is caused by a change in composition of the melt that London (2009) calls “fluxes”. The country rock and the widest portions of the dike (assumed to be nearest to the source of the melt) are granitic pegmatites and contain very large potassium feldspar crystals (about 6-8 cm across). These potassium feldspar megacrysts are most abundant in the portions of the dike that are neither at the edge nor in the center of the intrusive complex (Bateman and Chappell, 1979).

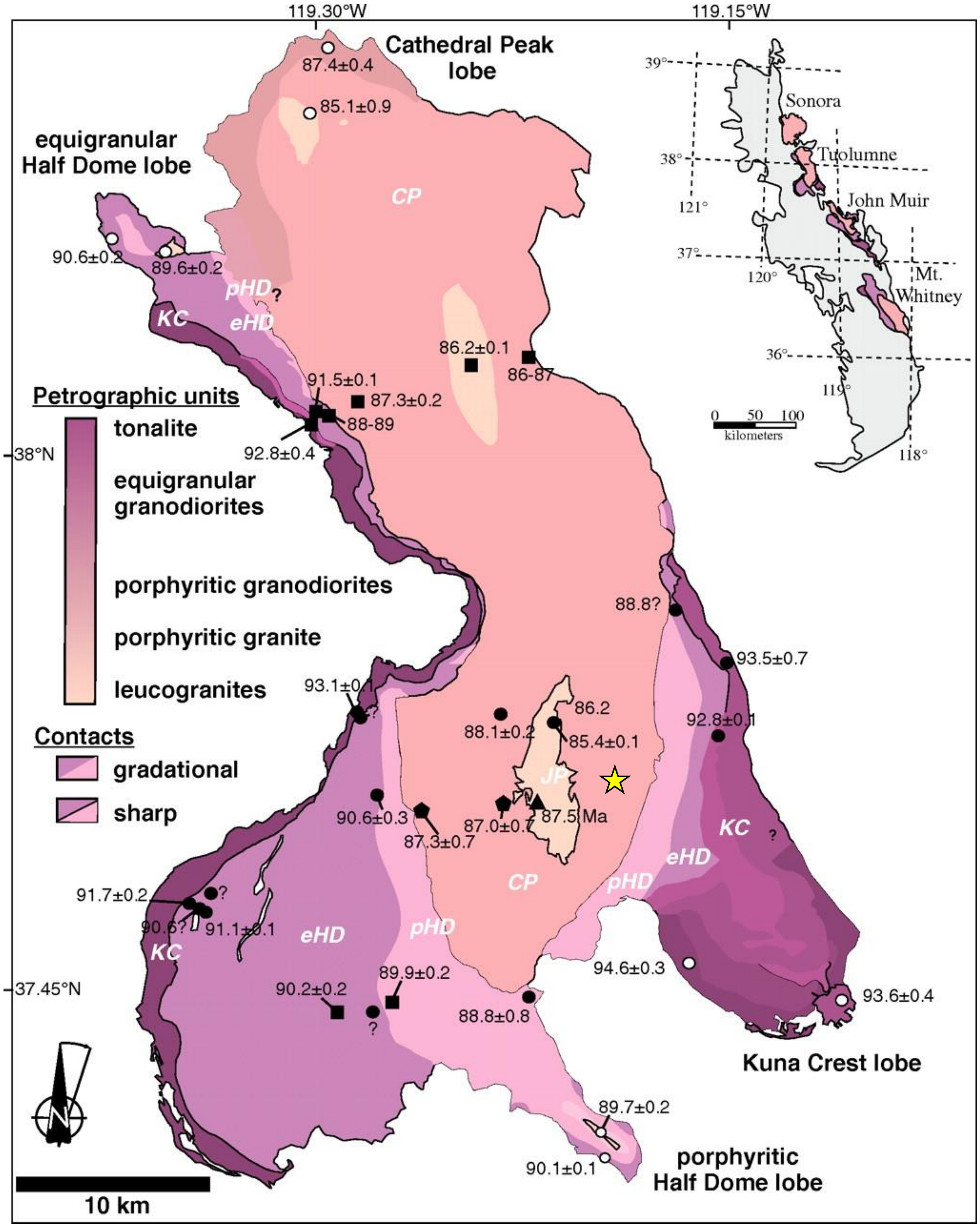

Figure 2. Map showing the Tuolumne Intrusive Complex, lithological and textural variations, along with U-Pb zircon ages displayed. Yellow star indicates the approximate location of Lembert Dome (modified from – Paterson et al., 2011).

This is another indication of fractionation in the Tuolumne Intrusive Complex and the dike on Lembert Dome. The potassium feldspar megacrysts are likely seen in the base of the dike as a result of log-jam, i.e. being picked up from the surrounding country rock as the dike was propagating through that area, and being locked in as the dike formed around them. Another variation seen in this intrusive complex is sharp versus gradational boundaries, which give some indication as to how the different regions formed. Some of the features of emplacement and original formation have been overwritten by later stages in its formation, by features like dikes and cracking, and by processes such as stoping (Žák et al., 2005).

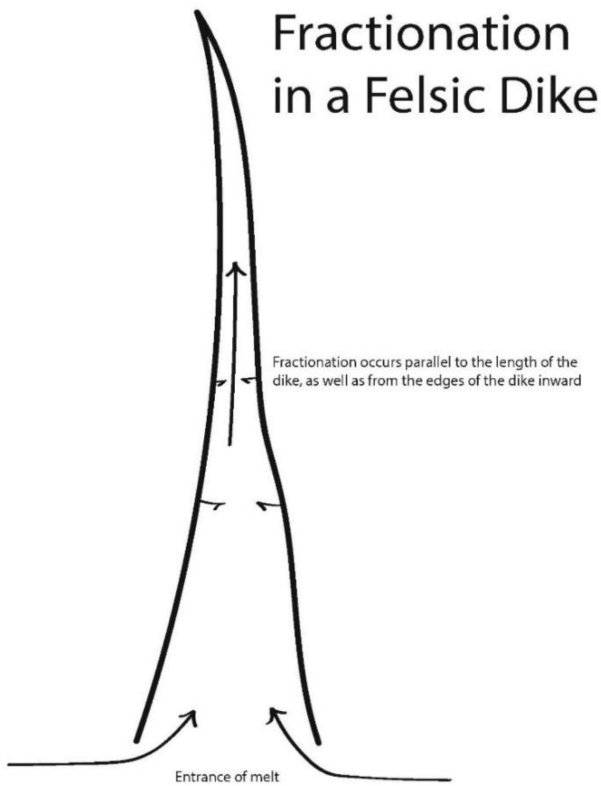

Figure 3. Schematic diagram of the idealized way a dike is fractionated along the length and across the width

For the last 10 million years, the area has been experiencing uplift that is widespread over much of the western United States. This has caused increased rates of erosion and changed the morphology of the area. Later, glaciers carved through Yosemite Valley, which exposed and polished many of the rocks, creating the current topography of the region, as well as the creation of the domes and valleys of the area, from a time period of about 2 million years ago until the end of the last glacial maximum.

Methodology

I began my project by doing background research on the Tuolumne Batholith, dike propagation, and characteristics of granites and granodiorites, as well as the principles of fractionation in igneous systems. Next, I looked at hand samples to identify the different textures seen in the dike and the surrounding country rock, and to characterize general mineralogy. The minerals evident in hand sample were potassium feldspar, plagioclase feldspar, quartz, biotite, and some small grains of titanite. There are also potassium feldspar megacrysts seen in some of the hand samples, which were only present in country rock and the wide end of the dike.

Following that, I examined 22 thin sections, recording mineralogy, grain size, texture, and any other notable features with a petrographic microscope. These thin sections were collected in 1995-96, and they are from four locations along the length of the dike (multiple samples were collected at each location), country rock, and two locations on an adjacent dike. They all had a mineralogy that was characteristic of a granodiorite. The proportions of the constituent minerals did vary slightly in different sections, but the main variation in the thin sections was textural. Some areas were very fine grained and equigranular, whereas other areas contained much larger grains in a fine grained matrix. The grain size, orientation of grains, zoning, and other microstructures give indication of how the minerals grew. Most thin sections had large grains that averaged 2-7 mm across, or small grains that were equigranular and less than 0.5 mm across. There was a general pattern that small grains were generally equigranular and large grains were highly fractured.

After examining the thin sections, I selected four thin sections and three epoxy mounts to analyze with EPMA, and focused on the following minerals: plagioclase, alkali feldspar, and biotite. These minerals were selected because they comprise the bulk of the rock (approximately 30%, 30%, and 10% respectively). Three of the thin sections are from the dike, as denoted by the green and red dots in the schematic found in appendix 4, and one thin section is from country rock found near the exposed source of the dike. I selected samples that were spread fairly evenly along the length of the dike, and two that were adjacent to one another, to enable me to compare the chemistry and mineralogy as it changes along the length of the dike. That data was worked through in Microsoft Excel to compute the mineral formulas for those analyses. A table of the mineral compositions can be found in appendix 2. Some analyses were not included in final results, because of totals that were too high or low for the values to be valid; these are red and italicized in the appendices tables. This could be a result of imperfections on the surface of the sample, the sample not being in focus when it was measured, the grain was not centered properly and adjacent grains were included in the measurement, to name a few potential sources for this error.

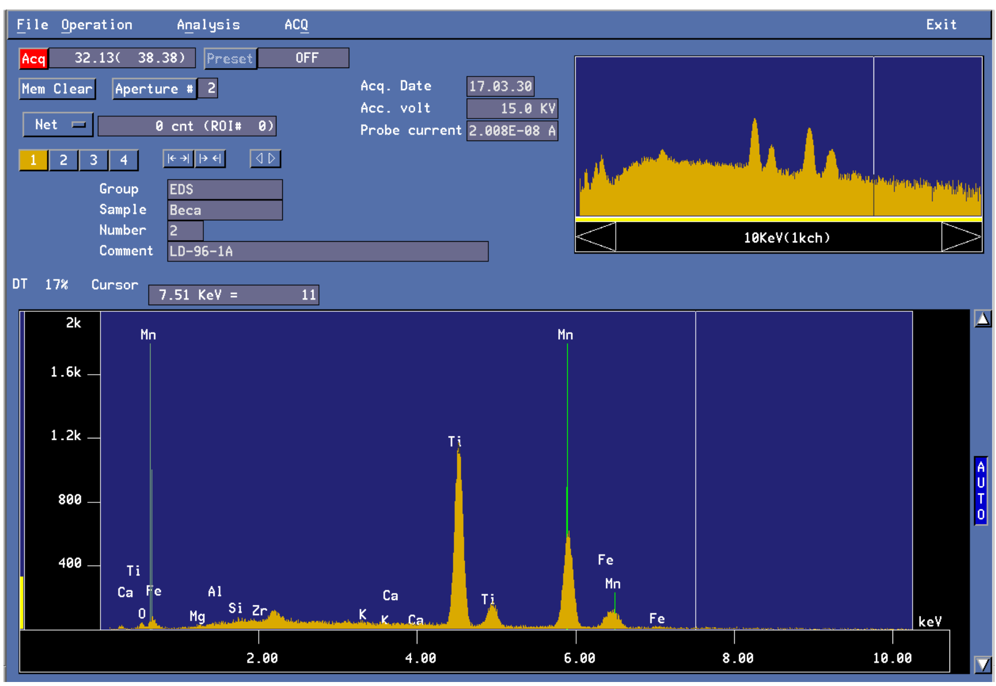

Figure 4. EDS spectra for an unknown mineral in thin section LD-96-1A, which shows peaks of x-rays and their corresponding elements emitted by the sample

The same samples were analyzed with LA-ICP-MS. Grains of plagioclase, chlorite, and biotite were analyzed for 35 different isotopes, including rare earth elements and some trace elements.

Electron Probe Microanalysis

I used an electron probe micro-analyzer to identify the mineral phases in thin section and epoxy mounts, and to determine the exact chemical composition of those phases. The electron probe micro-analyzer (EPMA) is a non-destructive method of doing chemical analysis. The model used is a Jeol JXA-8900R WD/ED Combo Micro-analyzer, located in the Advanced Imaging and Microscopy Lab. To begin, the samples are coated in a thin layer of carbon then loaded into the sample chamber, which is under vacuum. The sample is hit with an electron beam that is 5 microns wide on average. The beam is generated by using a tungsten filament with 15 kV accelerating potential. When the electrons hit the sample, they are most likely to hit the nucleus, since it is the largest part of the atom, causing some of the electrons to be "back scattered". Some of the electrons in the beam interact with inner shell electrons of the atoms, exciting them to a higher energy state. When these electrons fall back to a lower energy state, X-rays with a characteristic energy and wavelength are generated, and chemistry can therefore be determined using an EDS or WDS spectrometer.

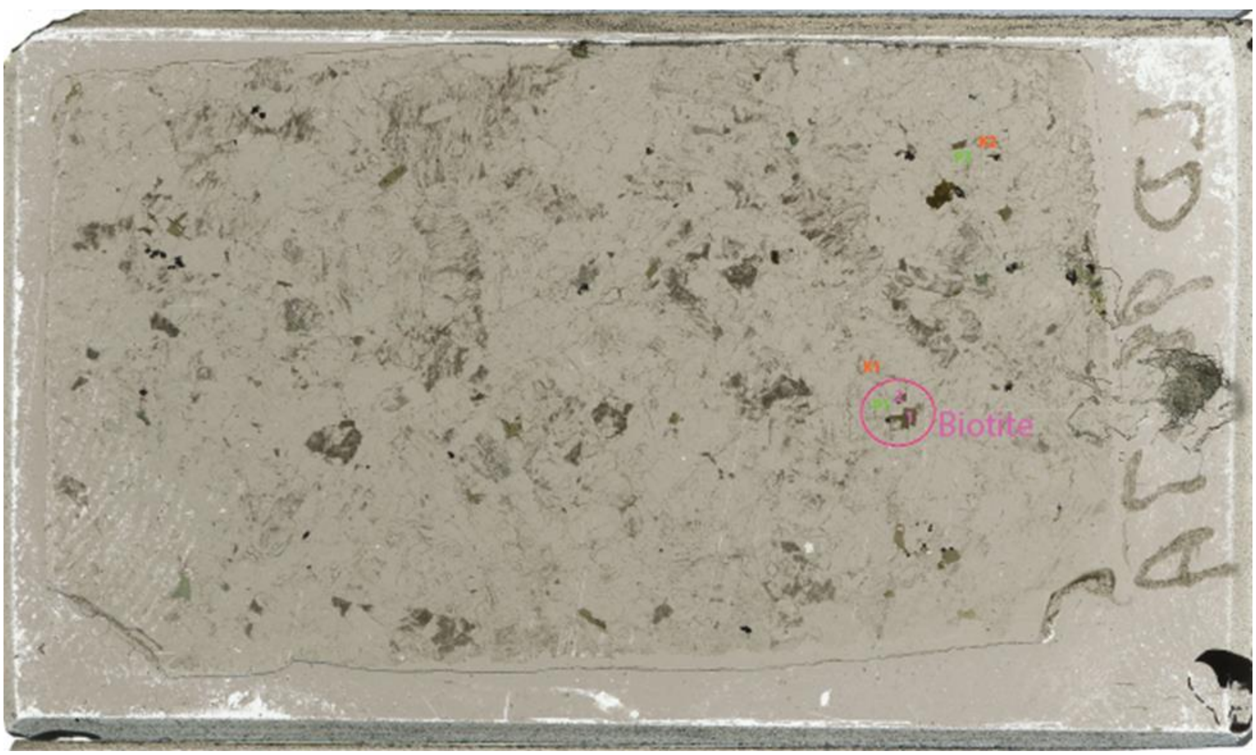

Figure 5. Thin section LD-96-7A that was examined using EPMA and LA-ICP-MS, with the six analyzed grains labeled in pink (biotite), green (plagioclase) and orange (potassium feldspar).

There are two primary types of data I collected from the EPMA: energy-dispersive spectroscopy (EDS) and wavelength-dispersive spectroscopy (WDS). EDS information can be found in real time while running the probe, which makes identification of minerals very quick. EDS is useful for identifying a mineral to determine if more analysis should be carried out on that grain. Determining more accurate composition requires WDS which takes several hours to collect. Mineral formulas were calculated from the composition data using Microsoft Excel by taking the weight percents (which is the metric the probe reports data in), dividing by the molar mass of the oxide, correcting for the number of oxygens found in that particular element, and multiplying by the cation-anion ratio for the given oxide. Uncertainties due to counting statistics have been accounted for and are included in appendix 2.

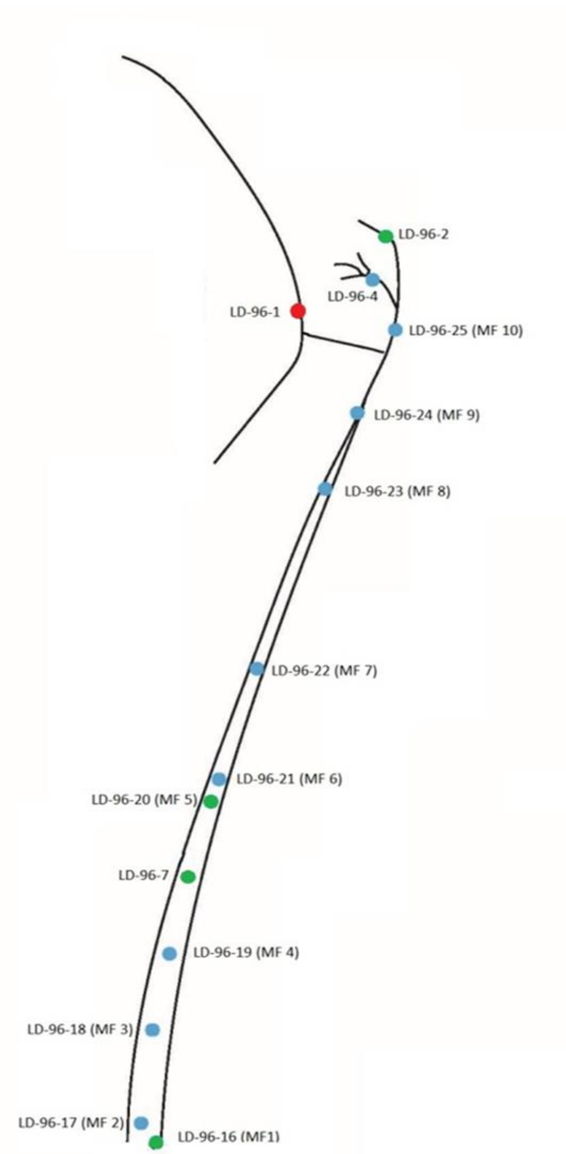

Figure 6. Schematic of the dike with sample site names. The green and red circles are locations of EPMA and LA-ICP-MS analyses. A more detailed version of this schematic is in appendix 4.

Laser Ablation Inductively Coupled Plasma Mass Spectrometry

I used laser ablation inductively coupled plasma mass spectrometry (LA-ICP-MS) for identifying the concentrations of 35 isotopes in thin sections LD-96-7A, LD-96-7G, and Y31 (country rock) and epoxy mounts MF1, MF5, and LD-96-2: Si^{29}, Ca^{43}, Sc^{45}, Ti^{47}, Mn^{55}, Zn^{67}, Ga^{69}, Ga^{71}, Rb^{85}, Sr^{88}, Y^{89}, Zr^{90}, Nb^{93}, In ^{115}, Sn^{117}, Ba^{137}, La^{139}, Ce^{140}, Pr^{141}, Nd^{146}, Sm^{147}, Eu^{151}, Eu^{153}, Gd^{157}, Tb^{159}, Dy^{163}, Ho^{165}, Er^{166}, Tm^{169}, Yb^{172}, Lu^{175}, Ta^{181}, Pb^{208}, Th^{232}, and U^{238}. LA-ICP-MS is a destructive and very sensitive method of analysis for use on solid and liquid samples; it is used to quantify the isotopes found in a sample to a value as exact as parts per billion.

Laser Ablation begins by loading the sample, either a thin section or an epoxy mount, into the stage. The sample is hit with a UV laser beam that ranges in size from 2 microns to 1200 microns wide, while helium gas flows across the top of the sample. The helium serves to carry the products of ablation to the mass spectrometer. The larger the beam that is used, the more material that is ablated, so there must be a balance between the size of the grain being ablated, the concentrations of the elements of interest, and having a small enough sample size to not oversaturate the mass spectrometer. The helium-sample mixture is combined with argon gas before reaching the argon plasma, where they are converted to ions. The ablated ions are now sent through a magnetic and electrical field, which will pull differently on atoms of varying atomic mass. The LA-ICP-MS can measure an ion of a particular atomic mass in milliseconds, and then adjusts the electrical or magnetic field to act on the next ion to be measured. A detector in the mass spectrometer is hit with electrons from the ions, which are multiplied as they pass through each layer of the detector. These detectors wear out over time as more electrons pass through them and the ablated portion of the sample is destroyed, which is why it is best to use the smallest sample necessary, while still being large enough to get a detectable value.

All of the values recorded by the LA-ICP-MS are given as ratios as compared to the standards used. The standards I used were NIST glass, a product manufactured specifically for use as a standard, and Hawaiian basaltic glass (called NIST610 and BHVO2g, respectively). These are used because they have known isotopic concentrations, after repeatedly being tested. Because the values are given as a ratio, data from the LA-ICP-MS has to be processed through another program, which can eliminate some background interference, calculate an average value for each isotope for the time the sample was being tested, and will convert the ratios into concentrations. The data generated in this process is found in appendix 3.

Results

Through optical microscopy, there is evident textural and mineralogical difference in various locations in the dike, which indicate fractionation during crystallization. Grains of garnet and tourmaline are present in the far end of the dike, but not anywhere in the country rock. Potassium feldspar megacrysts were only found in the widest portion of the dike, and are probably present due to “log jam” – being carried into the dike by melt as it formed, rather than forming primarily with the rest of the dike. The wide end of the dike is nearly indistinguishable from the surrounding country rock, meaning it came from a melt with similar composition and conditions of formation as the country rock. As observed moving along the 180 m length of the dike, the mineralogy and texture changes significantly; the distal end of the dike appears like a white stripe in the country rock, as seen in the photograph above.

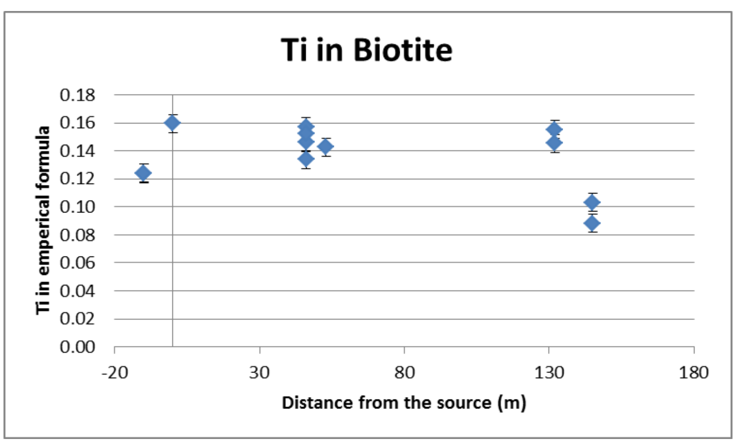

Figure 7. Graph of the amount of titanium in and the location in the dike. It is decreasing towards the distal end of the dike.

From EPMA, I saw some variation in the chemical compositions of the primary minerals of the rock. The chemistry of the major elements in the feldspars did not have any correlation to their location; graphs of the chemistry of cations along the length of the dike are found in appendix 5. Some grains of thorite or huttonite (solid solution end members with formula $(Th,U)SiO_4$) were verified with EDS which may indicate a large amount of thorium or uranium in samples that from the middle and narrow end of the dike. This is an indication of fractionation in the whole rock chemistry resulting in a higher concentration of thorium and uranium as the dike propagated through Lembert Dome. The titanium content of biotite as measured with EPMA and LA-ICP-MS decreased towards the distal end of the dike. Titanium content in biotite has been found to be a result of lower crystallization temperatures (Luhr 1984). The appearance of acicular radial biotite in the distal end of the dike is another indication of crystallization conditions that were different in the distal end of the dike as it propagated through the country rock (a photograph of the biotite "florettes" is seen below in figure 7, from sample LD-96-2). The habit of the biotite in this sample is evidence of undercooling; the dike is very narrow at this location, meaning it was propagating through relatively cool country rock.

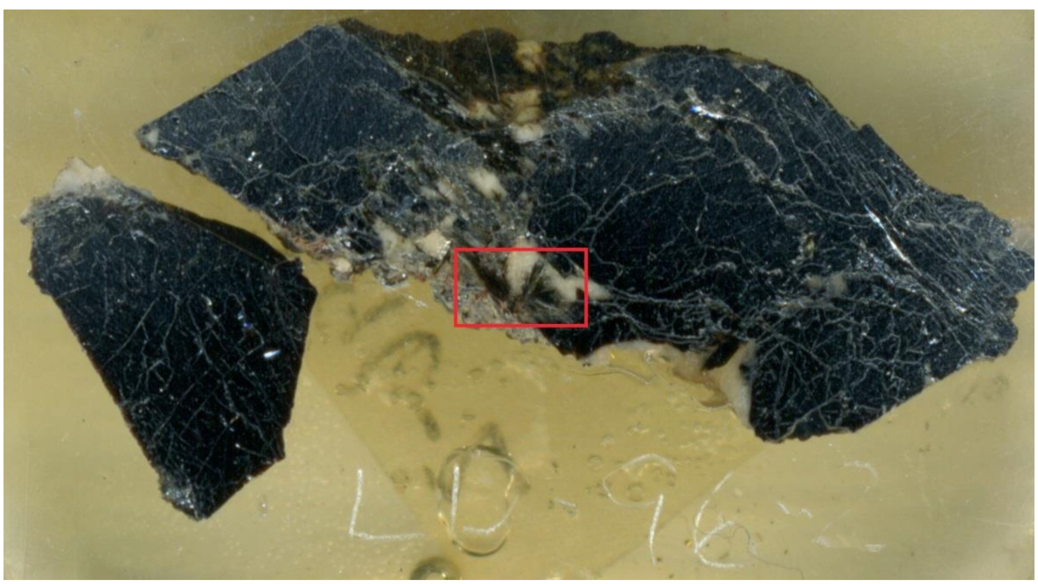

Figure 8. Biotite "florettes" found in the distal end of the dike.

LA-ICP-MS was performed on the same thin sections and epoxy mounts. The feldspars ablated very poorly because they are transparent and the UV laser cannot ablate transparent materials as well as opaque or colored samples. The feldspars' ablation percentages were rarely as high as 100% and instead often around 30-40%. That combined with the fact that there were not grains of both feldspars to analyze in many of the samples led me to focus on the trace and rare earth element concentrations of biotite. Biotite ablated very well (usually between 250-350%) and based on the works of Mahood and Hildreth (1983), is a useful mineral marker for showing evidence of fractionation. They found partition coefficients of major and minor elements in the early, middle, and late Bishop Tuff, similar to the way the dike is divided into "wide, middle, and narrow" for the samples I analyzed. There was increasing concentrations of all but two of the 35 isotopes measured with LA-ICP-MS (the exceptions were titanium and barium), although the amount of increase depended on the particular isotope. Figures 9 and 10 show two isotopes, and more are included in appendix 5.

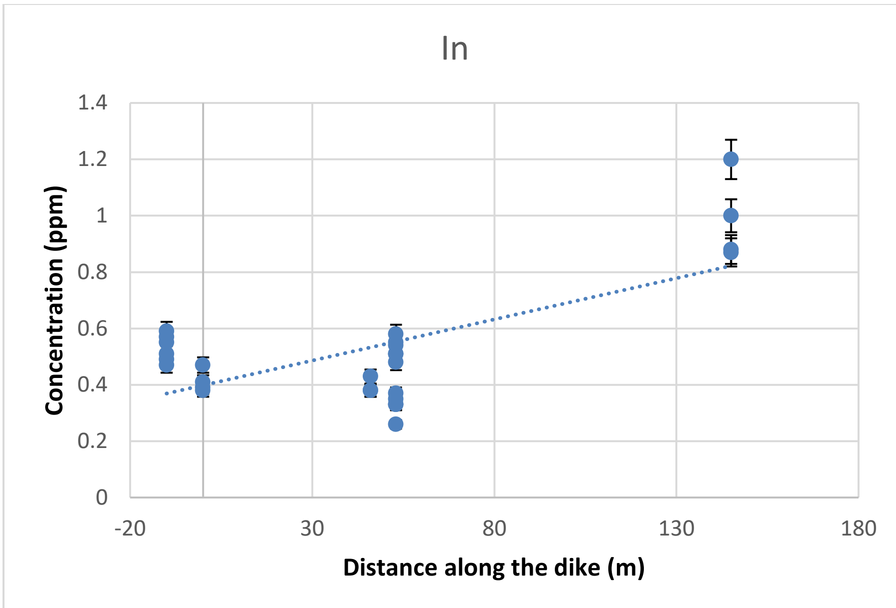

Figure 9. Indium 115 in biotite along the length of the dike, measured by LA-ICP-MS with error.

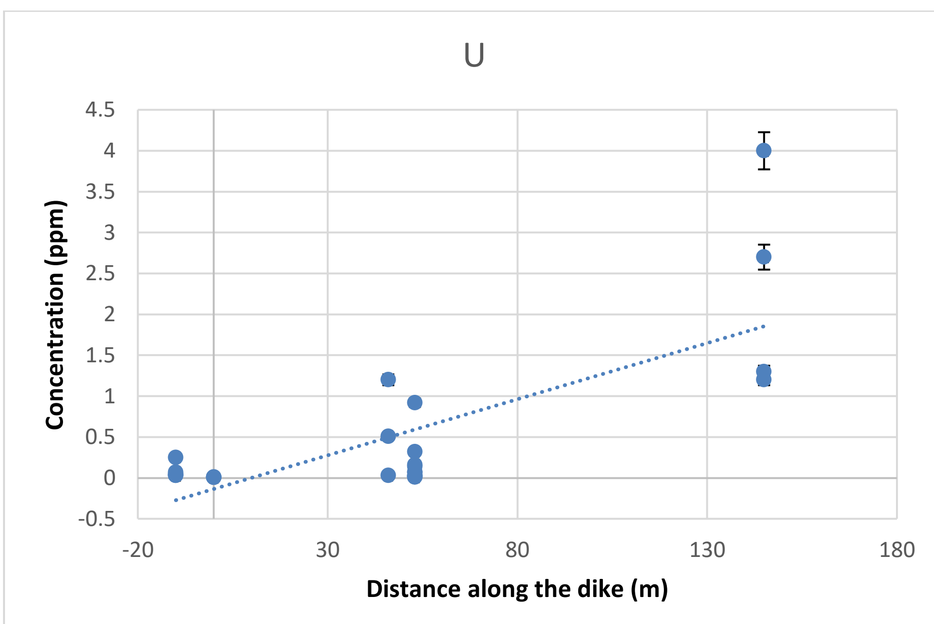

Figure 10. Uranium 238 in biotite along the length of the dike, measured by LA-ICP-MS with error.

Conclusions

After considering each method of analysis, previous research, and all of the other features that were examined, I have found the hypothesis that there is a variation in the chemistry of the major elements in the major rock-forming minerals of the dike (biotite, potassium feldspar, and plagioclase feldspar) and in the concentrations of the rare earth and trace elements to be related to the location along the length of the dike to be supported. There minerals present in narrower locations of the dike that were not present in the country rock. The correlation between the location and the chemistry of the rock is due to a difference in melt chemistry that resulted from fractionation, and also from different temperature conditions as the dike narrowed and propagated through colder country rock. This study measured variations of the chemistry of the biotite grains along the length of the dike, and also variations in its habit. Although there is evidence in biotite that there is a correlation between the chemistry of the dike and its location, this does not factor in the whole rock chemistry, which could further illustrate the link between location and chemistry resulting from fractionation in this dike.

Bibliography

- Bateman, P.C., and Chappell, B.W., 1979, Crystallization, fractionation, and solidification of the Tuolumne Intrusive Series, Yosemite National Park, California: Geological Society of America Bulletin, v. 90, p. 465, doi: 10.1130/0016-7606(1979)90<465:cfasot>2.0.co;2.
- Coleman, D.S., Gray, W., and Glazner, A.F., 2004, Rethinking the emplacement and evolution of zoned plutons: Geochronologic evidence for incremental assembly of the Tuolumne Intrusive Suite, California: Geology, v. 32, p. 433, doi: 10.1130/g20220.1.
- Kretz, R., 1983, Symbols for Rock Forming Minerals: American Mineralogist, v. 68, p. 277–278.
- London, D., 2009, The Origin Of Primary Textures In Granitic Pegmatites: The Canadian Mineralogist, v. 47, p. 697–724, doi: 10.3749/canmin.47.4.697.
- Luhr, J.F., Charmichael, I.S.E., and Varekamp, J.C., 1984, The 1982 eruptions of El Chichón Volcano (Chiapas, Mexico): Character of the eruptions, ash-fall deposits, and gasphase: Journal of Volcanology and Geothermal Research, v. 23, p. 39–68, doi: 10.1016/0377-0273(84)90056-8.
- Mahood, G., and Hildreth, W., 1983, Large partition coefficients for trace elements in high-silica rhyolites: Geochimica et Cosmochimica Acta, v. 47, p. 11–30, doi: 10.1016/0016-7037(83)90087-x.
- Paterson, S.R., Okaya, D., Memeti, V., Economos, R., and Miller, R.B., 2011, Magma addition and flux calculations of incrementally constructed magma chambers in continental margin arcs: Combined field, geochronologic, and thermal modeling studies: Geosphere, v. 7, p. 1439–1468, doi: 10.1130/ges00696.1.
- Žák, J.C.C.A.D., and Paterson, S.R., 2005, Characteristics of internal contacts in the Tuolumne Batholith, central Sierra Nevada, California (USA): Implications for episodic emplacement and physical processes in a continental arc magma chamber: Geological Society of America Bulletin, v. 117, p. 1242-1255, doi: 10.1130/b25558.1.

Appendix 1

Photograph of Lembert Dome. The approximate location of the dike that is the focus of this study is denoted by the arrow. (Source: https://upload.wikimedia.org/wikipedia/commons/6/68/Yosemite-tuolumne_meadows-lembert_dome_1.jpeg)

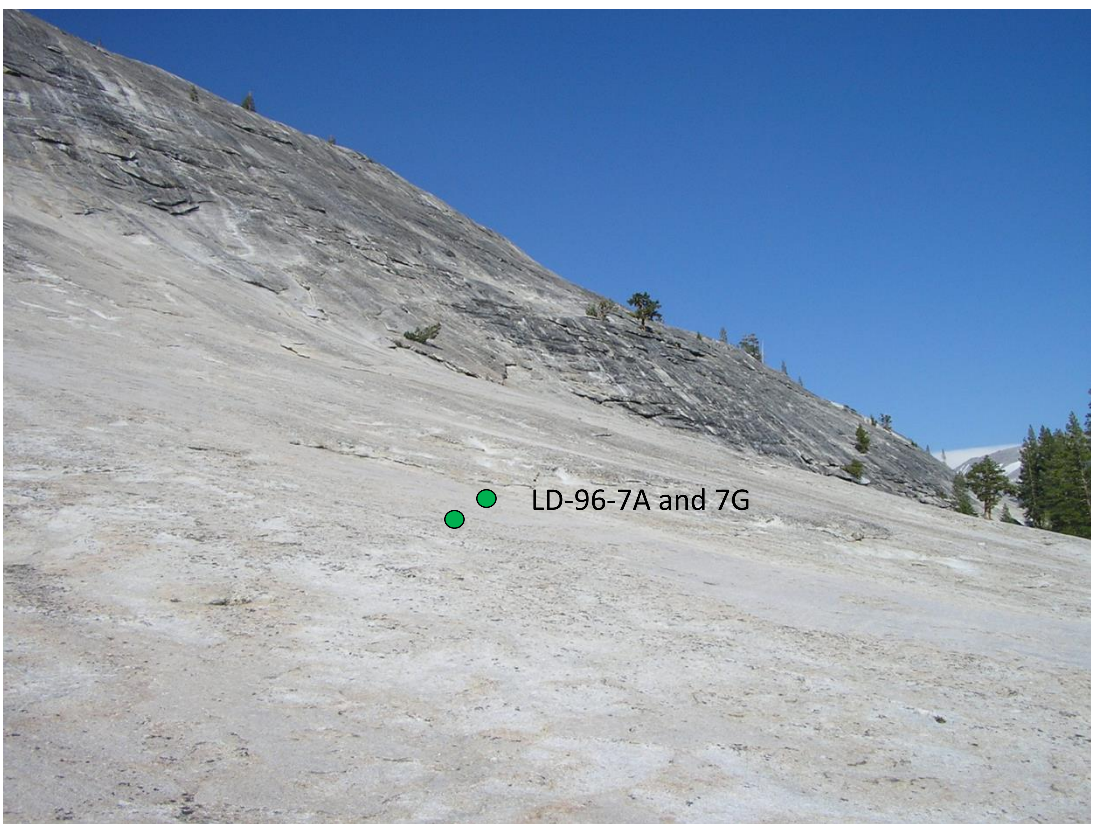

Wide end of the dike with glacial polish, photo modified from Philip Piccoli

Appendix 2

Composition of Plagioclase Feldspar (wt %)

	SiO_2	TiO_2	Al_2O_3	FeO	MnO	MgO	CaO	Na_2O	K_2O	Total
Y-31 Host CP P 1.1	62.91	0.04	23.37	0.17	0.02	0.00	4.76	8.83	0.25	100.34
Y-31 Host CP P 1.2	62.48	0.00	23.87	0.12	0.00	0.00	5.11	8.82	0.14	100.54
Y-31 Host CP P 1.3	62.12	0.00	24.05	0.18	0.00	0.00	5.11	8.54	0.21	100.20
Y-31 Host CP P 2.1	64.00	0.01	23.24	0.15	0.00	0.00	4.28	9.11	0.17	100.95
Y-31 Host CP P 2.2	64.03	0.00	23.07	0.16	0.00	0.00	3.97	9.43	0.17	100.83
Y-31 Host CP P 2.3	64.24	0.00	22.85	0.17	0.00	0.00	3.99	9.46	0.17	100.88
MF-5-2 P 1.1	66.29	0.01	22.20	0.15	0.00	0.01	2.97	9.50	0.29	101.42
MF-5-2 P 1.2	66.88	0.00	22.56	0.19	0.00	0.02	3.07	9.57	0.21	102.50
MF-5-2 P 1.3	65.98	0.00	22.01	0.18	0.00	0.00	2.99	9.53	0.32	101.01
LD-96-7A P 1.1	64.30	0.00	22.29	0.13	0.00	0.00	3.26	9.27	0.42	99.67
LD-96-7A P 1.2	65.37	0.00	22.50	0.15	0.00	0.01	3.23	9.82	0.17	101.26
LD-96-7A P 1.3	64.39	0.00	22.62	0.15	0.03	0.00	3.49	9.65	0.27	100.60
LD-96-7A P 2.1	65.16	0.00	22.19	0.15	0.00	0.00	3.23	9.61	0.46	100.79
LD-96-7A P 2.2	65.11	0.00	22.21	0.12	0.01	0.00	3.18	9.54	0.42	100.58
LD-96-7A P 2.3	64.99	0.00	22.25	0.13	0.00	0.00	3.06	9.60	0.44	100.47
LD-96-7G P 1.1	82.69	0.00	11.45	0.03	0.00	0.00	1.00	5.05	0.06	100.29
LD-96-7G P 1.2	67.60	0.00	21.32	0.07	0.00	0.02	2.03	10.25	0.10	101.39
LD-96-7G P 1.3	65.84	0.00	21.60	0.11	0.00	0.02	2.44	10.04	0.13	100.18
LD-96-7G P 2.1	65.18	0.04	22.15	0.15	0.01	0.02	3.07	9.74	0.39	100.74
LD-96-7G P 2.2	65.24	0.00	22.10	0.15	0.03	0.00	3.03	9.63	0.40	100.57
LD-96-7G P 2.3	63.41	0.01	22.97	0.14	0.02	0.01	3.16	9.51	0.25	99.48
LD-96-1A P 1.1	68.45	0.00	20.49	0.09	0.00	0.00	0.93	10.04	0.06	100.06
LD-96-1A P 1.2	69.16	0.02	20.26	0.07	0.00	0.00	0.66	10.60	0.11	100.89
LD-96-1A P 1.3	67.70	0.00	21.30	0.16	0.03	0.00	1.86	9.67	0.58	101.29
LD-96-1A P 1.4	68.09	0.00	21.07	0.14	0.00	0.03	1.83	9.09	1.02	101.28

	SiO_2	TiO_2	Al_2O_3	FeO	MnO	MgO	CaO	Na_2O	K_2O	Total
LD-96-1A P 2.1	55.89	0.00	16.87	0.10	0.01	0.02	0.45	6.48	3.14	82.95
LD-96-1A P 2.2	68.04	0.00	20.62	0.03	0.00	0.02	0.86	10.29	0.17	100.03
LD-96-1A P 2.3	67.33	0.00	21.66	0.11	0.00	0.01	2.01	10.01	0.18	101.30
LD-96-1A P 2.4	67.63	0.00	21.75	0.05	0.01	0.00	2.06	9.85	0.12	101.47
LD-96-2 P 1.1 (in Tur)	67.31	0.00	20.88	0.01	0.01	0.00	0.38	10.93	0.07	99.58
LD-96-2 P 1.1 (in Tur)	68.45	0.00	19.88	0.04	0.03	0.00	0.28	11.78	0.08	100.53
LD-96-2 P 1.1 (in Tur)	67.68	0.00	19.24	0.05	0.00	0.00	0.23	11.51	0.08	98.79
LD-96-2 P 1.1 (in Tur)	69.02	0.01	19.61	0.07	0.02	0.00	0.08	11.52	0.06	100.40
LD-96-2 P 2.1 (in Tur)	68.81	0.00	19.86	0.03	0.03	0.00	0.46	11.34	0.08	100.61
LD-96-2 P 2.1 (in Tur)	69.23	0.00	20.09	0.12	0.00	0.00	0.55	11.23	0.09	101.31
LD-96-2 P 2.1 (in Tur)	68.51	0.00	19.73	0.10	0.00	0.00	0.30	11.62	0.07	100.33

Composition of Potassium Feldspar (wt %)

	SiO_2	TiO_2	Al_2O_3	FeO	MnO	MgO	CaO	Na_2O	K_2O	Total
Y-31 Host CP K 1.1	65.49	0.01	18.66	0.10	0.00	0.00	0.00	0.77	15.58	100.61
Y-31 Host CP K 1.2	65.17	0.04	18.42	0.07	0.01	0.00	0.00	0.87	15.36	99.95
Y-31 Host CP K 1.3	65.61	0.00	18.68	0.07	0.00	0.00	0.00	0.99	15.28	100.63
Y-31 Host CP K 2.1	65.87	0.02	18.71	0.02	0.01	0.00	0.00	0.53	15.91	101.07
Y-31 Host CP K 2.2	65.24	0.00	18.55	0.02	0.00	0.00	0.01	0.56	15.77	100.14
Y-31 Host CP K 2.3	64.82	0.01	18.90	0.02	0.02	0.00	0.02	0.51	15.48	99.77
MF-1 K 1.1	66.09	0.00	18.70	0.08	0.00	0.00	0.03	1.20	14.87	100.97
MF-1 K 1.2	66.06	0.00	18.75	0.07	0.02	0.00	0.05	1.17	14.63	100.75
MF-1 K 1.3	65.98	0.04	18.66	0.10	0.03	0.00	0.02	1.25	14.51	100.58
MF-1 K 1.4	65.64	0.01	18.52	0.10	0.02	0.00	0.03	0.91	15.30	100.52
MF-1 K 2.1	66.13	0.00	18.58	0.05	0.00	0.00	0.03	1.09	15.01	100.89
MF-1 K 2.2	66.19	0.00	18.59	0.09	0.00	0.00	0.02	1.01	15.25	101.15
LD-96-7A K 1.1	65.50	0.00	18.35	0.06	0.01	0.00	0.00	0.74	15.61	100.27
LD-96-7A K 1.2	65.41	0.03	18.81	0.09	0.02	0.00	0.00	0.48	15.72	100.57
LD-96-7A K 1.3	65.13	0.00	18.83	0.08	0.00	0.00	0.00	0.40	15.49	99.93
LD-96-7A K 2.1	65.58	0.00	18.61	0.04	0.02	0.00	0.02	0.46	15.89	100.61
LD-96-7A K 2.2	65.79	0.04	18.39	0.07	0.01	0.00	0.00	0.77	15.36	100.43
LD-96-7A K 2.3	65.35	0.00	18.87	0.01	0.00	0.00	0.02	0.32	15.92	100.49
LD-96-7G K 1.1	65.62	0.00	18.61	0.08	0.00	0.00	0.02	0.83	15.16	100.32
LD-96-7G K 1.2	65.52	0.00	18.59	0.09	0.00	0.00	0.02	0.59	15.70	100.51
LD-96-7G K 1.3	65.53	0.00	18.83	0.07	0.00	0.00	0.01	1.25	14.71	100.40
LD-96-7G K 2.1	65.46	0.00	18.46	0.07	0.00	0.00	0.03	0.96	15.06	100.03
LD-96-7G K 2.2	65.55	0.00	18.57	0.08	0.00	0.00	0.00	0.90	15.19	100.29
LD-96-7G K 2.3	65.13	0.01	18.51	0.07	0.00	0.00	0.01	0.78	15.12	99.63
LD-96-1A K 1.1	65.57	0.01	18.85	0.16	0.02	0.00	0.02	0.96	15.30	100.89
LD-96-1A K 1.2	65.22	0.00	18.72	0.14	0.00	0.00	0.03	0.73	15.60	100.45

	SiO_2	TiO_2	Al_2O_3	FeO	MnO	MgO	CaO	Na_2O	K_2O	
LD-96-1A K 1.3	65.16	0.00	18.80	0.12	0.01	0.00	0.02	0.62	15.92	100.65
LD-96-1A K 1.4	65.21	0.00	18.82	0.11	0.00	0.00	0.02	0.61	15.52	100.29
LD-96-1A-K 2.1	*57.16*	*0.00*	*24.96*	*0.19*	*0.00*	*0.03*	*0.19*	*1.05*	*13.23*	*96.80*
LD-96-1A-K 2.2	63.68	0.00	19.52	0.10	0.01	0.00	0.06	1.16	14.61	99.13
LD-96-1A-K 2.3	65.12	0.00	18.41	0.09	0.00	0.00	0.02	0.84	15.71	100.19

Composition of Biotite (wt %)

	SiO_2	TiO_2	Al_2O_3	FeO	MnO	MgO	CaO	Na_2O	K_2O	Total
Y-31 Host CP Bt 1.1	37.78	2.42	14.67	17.35	1.04	13.13	0.02	0.11	9.43	95.94
Y-31 Host CP Bt 1.2	37.87	2.27	14.54	17.41	1.11	13.00	0.00	0.10	9.70	96.00
Y-31 Host CP Bt 1.3	38.23	1.89	14.85	16.75	1.06	13.78	0.06	0.11	9.23	95.95
Y-31 Host CP Bt 2.1	37.70	2.19	14.67	17.57	1.06	13.18	0.01	0.11	9.61	96.10
Y-31 Host CP Bt 2.2	37.96	2.26	14.63	17.45	1.05	13.34	0.06	0.10	9.60	96.45
Y-31 Host CP Bt 2.3	37.88	2.15	15.07	16.96	1.09	13.12	0.00	0.09	9.71	96.07
MF-1 Bt 1.1	38.60	2.84	14.19	16.10	1.04	13.82	0.00	0.09	9.35	96.03
MF-1 Bt 1.2	38.76	2.94	14.00	15.69	1.03	13.90	0.00	0.06	9.35	95.72
MF-1 Bt 1.3	38.96	2.83	14.08	15.55	1.05	13.91	0.00	0.08	9.12	95.59
MF-1 Bt 1.4	38.64	2.78	13.94	15.81	1.04	13.64	0.00	0.06	9.29	95.20
MF-1 Bt 1.5	38.24	2.79	14.00	15.67	0.99	13.65	0.01	0.09	8.89	94.34
MF-5-2 Bt 1.1	37.85	2.47	15.14	16.62	1.04	12.63	0.00	0.05	9.46	95.26
MF-5-2 Bt 1.2	38.36	2.40	14.37	16.02	0.97	13.29	0.00	0.05	9.39	94.84
MF-5-2 Bt 1.3	38.10	2.46	14.78	16.34	1.01	12.88	0.00	0.05	9.57	95.19
MF-5-2 Bt 1.4	38.09	2.74	14.40	16.44	1.04	13.01	0.00	0.03	9.55	95.30
LD-96-7A Bt 1.1	37.86	2.92	14.76	16.52	1.10	13.13	0.00	0.08	9.55	95.92
LD-96-7A Bt 1.2	38.33	2.85	15.22	15.91	1.20	12.52	0.00	0.04	9.74	95.81
LD-96-7A Bt 1.3	38.65	2.62	14.69	15.84	1.08	13.34	0.00	0.06	9.64	95.92
LD-96-7A Bt 2.1	38.46	2.37	14.67	16.43	1.14	13.46	0.02	0.07	9.55	96.17
LD-96-7A Bt 2.2	38.26	2.20	15.53	16.00	1.08	13.57	0.09	0.17	8.98	95.88
LD-96-7A Bt 2.3	37.60	2.58	15.36	16.66	1.17	13.08	0.00	0.09	9.15	95.69
LD-96-7G Bt 1.1	38.27	2.64	14.69	15.30	0.96	13.40	0.00	0.06	9.45	94.77
LD-96-7G Bt 1.2	38.05	2.62	14.70	16.01	0.97	13.39	0.00	0.09	9.43	95.27
LD-96-7G Bt 1.3	38.18	2.50	14.82	16.04	0.97	13.42	0.00	0.02	9.53	95.48
LD-96-7G Bt 2.1	38.35	2.73	14.62	16.38	0.96	13.80	0.00	0.11	9.48	96.43
LD-96-7G Bt 2.2	38.22	2.73	14.60	16.45	0.97	13.51	0.00	0.06	9.48	96.02

	SiO_2	TiO_2	Al_2O_3	FeO	MnO	MgO	CaO	Na_2O	K_2O	Total
LD-96-7G Bt 2.3	38.62	2.73	14.97	16.41	1.03	13.71	0.04	0.11	9.27	96.89
LD-96-1A Bt 1.1	38.26	2.44	13.34	15.75	2.59	12.41	0.09	0.10	9.30	94.28
LD-96-1A Bt 1.2	38.57	2.58	13.46	15.61	2.71	12.52	0.02	0.11	9.66	95.23
LD-96-1A Bt 1.3	38.49	2.62	13.44	15.86	2.75	12.73	0.00	0.11	9.55	95.54
LD-96-1A B 2.1	37.39	2.71	14.76	15.36	1.31	12.45	0.13	0.09	9.27	93.47
LD-96-1A B 2.2	38.67	2.75	14.30	15.93	1.33	13.58	0.00	0.10	9.48	96.14
LD-96-1A B 2.3	38.49	2.74	14.22	15.78	1.20	13.07	0.05	0.13	9.46	95.14
LD-96-2 Bt Florettes 1.1	38.60	1.65	15.08	16.30	1.20	13.05	0.03	0.05	9.11	95.08
LD-96-2 Bt Florettes 1.2	37.59	1.81	16.79	17.19	1.07	11.33	0.15	0.05	7.35	93.33
LD-96-2 Bt Florettes 1.3	38.01	1.92	15.93	16.43	1.20	12.36	0.10	0.07	8.90	94.92
LD-96-2 Bt Florettes 1.4	38.81	1.85	15.70	15.62	1.12	12.64	0.09	0.05	8.77	94.65
LD-96-2 Bt Florettes 1.5	37.72	1.85	15.43	16.35	1.18	12.95	0.16	0.10	8.49	94.22
LD-96-2 Bt 2.1	37.69	1.56	16.20	16.81	1.22	12.93	0.19	0.07	7.97	94.64
LD-96-2 Bt 2.2	*36.87*	*1.51*	*15.67*	*16.18*	*1.17*	*12.27*	*0.04*	*0.05*	*8.27*	*92.03*

Uncertainties due to counting statistics

Plagioclase and potassium feldspar

	Si	Ti	Al	Fe	Mn	Mg	Ca	Na	K
Y-31 Host CP Ksp 1.1	0.21	234.82	0.38	18.50	1491.65	100.00	100.00	2.95	0.47
Y-31 Host CP Ksp 1.2	0.21	51.32	0.38	24.84	134.38	100.00	231.52	2.69	0.47
Y-31 Host CP Ksp 1.3	0.21	100.00	0.38	27.66	100.00	100.00	1447.99	2.55	0.47
Y-31 Host CP Plag 1.1	0.21	57.86	0.34	10.63	85.09	253.88	0.75	0.75	4.77
Y-31 Host CP Plag 1.2	0.22	100.00	0.34	15.04	585.49	481.90	0.72	0.75	7.81
Y-31 Host CP Plag 1.3	0.22	442.50	0.34	10.47	100.00	185.36	0.72	0.77	5.76
Y-31 Host CP Plag 2.1	0.21	206.84	0.34	11.98	100.00	350.00	0.80	0.74	6.93
Y-31 Host CP Plag 2.2	0.21	100.00	0.35	11.18	100.00	100.00	0.82	0.73	6.32
Y-31 Host CP Plag 2.3	0.21	100.00	0.35	11.36	100.00	100.00	0.82	0.73	6.49
Y-31 Host CP Ksp 2.1	0.20	105.38	0.38	94.02	178.71	100.00	100.00	3.68	0.46
Y-31 Host CP Ksp 2.2	0.21	100.00	0.38	115.95	100.00	100.00	107.53	3.65	0.46
Y-31 Host CP Ksp 2.3	0.21	182.53	0.38	100.32	105.99	100.00	57.31	3.88	0.47
MF-1 Kspar 1.1	0.20	100.00	0.37	22.19	100.00	100.00	36.10	2.25	0.47
MF-1 Kspar 1.2	0.20	100.00	0.37	26.52	69.16	100.00	23.69	2.27	0.48
MF-1 Kspar 1.3	0.21	54.66	0.38	18.80	66.33	100.00	62.35	2.22	0.49
MF-1 Kspar 1.4	0.21	252.11	0.39	18.95	73.65	100.00	43.43	2.68	0.48
MF-1 Kspar 2.1	0.21	893.17	0.38	36.76	100.00	100.00	35.29	2.45	0.48
MF-1 Kspar 2.2	0.21	1165.79	0.38	19.49	100.00	100.00	56.97	2.52	0.48
MF-5-2 Plag 1.1	0.21	181.48	0.36	12.30	577.23	83.04	1.00	0.74	4.58
MF-5-2 Plag 1.2	0.21	1165.78	0.36	9.09	100.00	46.65	0.97	0.74	5.90
MF-5-2 Plag 1.3	0.21	100.00	0.36	10.38	100.00	100.00	0.98	0.73	4.27
LD-96-7A Pl 1.1	0.21	100.00	0.35	13.96	100.00	1447.99	0.93	0.74	3.49
LD-96-7A Pl 1.2	0.21	591.19	0.35	12.23	100.00	57.70	0.94	0.71	6.44
LD-96-7A Pl 1.3	0.21	100.00	0.35	11.80	59.38	280.24	0.89	0.72	4.55

LD-96-7A Ksp 1.1	0.21	903.30	0.38	27.09	295.64	100.00	100.00	2.98	0.47
LD-96-7A Ksp 1.2	0.21	64.14	0.38	18.83	71.90	100.00	100.00	4.07	0.46
LD-96-7A Ksp 1.3	0.21	597.62	0.38	21.05	100.00	100.00	100.00	4.42	0.47
LD-96-7A Ksp 2.1	0.21	100.00	0.38	46.44	105.22	100.00	55.14	4.18	0.46
LD-96-7A Ksp 2.2	0.21	55.48	0.38	25.43	227.02	100.00	100.00	2.98	0.47
LD-96-7A Ksp 2.3	0.21	3483.01	0.38	145.87	100.00	100.00	66.61	5.41	0.46
LD-96-7A Plag 2.1	0.21	437.16	0.35	13.45	100.00	100.00	0.93	0.72	3.24
LD-96-7A Plag 2.2	0.21	100.00	0.35	16.11	155.33	100.00	0.94	0.72	3.43
LD-96-7A Plag 2.3	0.21	100.00	0.35	14.46	100.00	100.00	0.96	0.72	3.43
LD-96-7G Plag 1.1	0.18	100.00	0.49	49.85	100.00	100.00	1.86	1.01	14.41
LD-96-7G Plag 1.2	0.21	100.00	0.36	23.63	100.00	46.65	1.21	0.69	9.94
LD-96-7G Plag 1.3	0.21	100.00	0.36	16.52	100.00	36.29	1.08	0.70	8.11
LD-96-7G Ksp 1.1	0.21	100.00	0.38	23.49	100.00	100.00	51.43	2.81	0.47
LD-96-7G Ksp 1.2	0.21	100.00	0.38	20.57	100.00	100.00	62.65	3.58	0.46
LD-96-7G Ksp 1.3	0.21	100.00	0.38	26.65	100.00	100.00	129.01	2.23	0.48
LD-96-7G Plag 2.1	0.21	61.59	0.35	11.80	193.56	53.68	0.95	0.71	3.60
LD-96-7G Plag 2.2	0.21	100.00	0.35	12.56	61.79	4062.51	0.96	0.72	3.43
LD-96-7G Plag 2.3	0.21	313.21	0.35	13.01	75.53	119.86	0.94	0.72	4.86
LD-96-7G KSP 2.1	0.21	100.00	0.38	26.38	100.00	100.00	42.60	2.60	0.47
LD-96-7G KSP 2.2	0.21	100.00	0.38	22.99	437.29	100.00	100.00	2.62	0.47
LD-96-7G KSP 2.3	0.21	269.44	0.38	26.54	100.00	100.00	189.78	2.93	0.47
LD-96-2 Plag (in Tur) 1.1	0.21	100.00	0.37	220.54	308.52	100.00	3.76	0.68	13.97
LD-96-2 Plag (in Tur) 1.2	0.21	100.00	0.38	45.72	53.81	175.51	4.71	0.66	13.08
LD-96-2 Plag (in Tur) 1.3	0.21	100.00	0.39	30.97	100.00	100.00	5.70	0.66	11.43
LD-96-2 Plag (in Tur) 1.4	0.21	422.95	0.38	23.13	72.74	170.27	14.92	0.66	15.56
LD-96-2 Plag (in Tur) 2.1	0.21	100.00	0.38	56.29	62.57	100.00	3.15	0.67	11.99
LD-96-2 Plag (in Tur) 2.2	0.21	847.80	0.38	14.10	100.00	1060.07	2.77	0.67	10.61
LD-96-2 Plag (in Tur) 2.3	0.21	100.00	0.38	17.24	100.00	100.00	4.55	0.66	13.46

Biotite

	Si	Ti	Al	Fe	Mn	Mg	Ca	Na	K
Y-31 Host CP Bt 1.1	0.28	1.8	0.47	0.46	2.8	0.51	63.69	15.13	0.6
Y-31 Host CP Bt 1.2	0.28	1.93	0.47	0.46	2.66	0.51	100	15.36	0.59
Y-31 Host CP Bt 1.3	0.28	2.15	0.47	0.47	2.77	0.49	21.16	14.96	0.6
Y-31 Host CP Bt 2.1	0.28	1.98	0.47	0.46	2.73	0.51	110.42	14.78	0.59
Y-31 Host CP Bt 2.2	0.28	1.94	0.47	0.46	2.84	0.5	19.74	15.96	0.59
Y-31 Host CP Bt 2.3	0.28	2	0.46	0.47	2.74	0.51	100	16.49	0.59
MF-1 Bt 1.1	0.28	1.67	0.49	0.49	2.81	0.5	100	16.02	0.61
MF-1 Bt 1.2	0.28	1.63	0.49	0.5	2.9	0.5	100	26.27	0.61
MF-1 Bt 1.3	0.28	1.69	0.49	0.5	2.73	0.5	100	18.43	0.61
MF-1 Bt 1.4	0.28	1.71	0.49	0.49	2.86	0.5	100	25.77	0.61
MF-1 Bt 1.5	0.29	1.71	0.49	0.49	2.94	0.5	90.94	15.82	0.62
MF-5-2 Bt 1.1	0.29	1.84	0.47	0.48	2.83	0.52	100	27.06	0.6
MF-5-2 Bt 1.2	0.28	1.87	0.48	0.49	2.96	0.51	100	32.5	0.61
MF-5-2 Bt 1.3	0.29	1.84	0.47	0.48	2.9	0.52	100	31.41	0.6
MF-5-2 Bt 1.4	0.29	1.69	0.48	0.48	2.87	0.51	100	46.26	0.6
LD-96-7A Bt 1.1	0.28	1.62	0.47	0.47	2.7	0.51	100	18.28	0.59
LD-96-7A Bt 1.2	0.28	1.66	0.46	0.48	2.52	0.52	100	38.98	0.59
LD-96-7A Bt 1.3	0.28	1.74	0.47	0.49	2.78	0.5	100	23.27	0.59
LD-96-7A Bt 2.1	0.28	1.84	0.47	0.48	2.65	0.5	72.68	23.48	0.59
LD-96-7A Bt 2.2	0.28	1.96	0.46	0.48	2.75	0.5	13.55	10.45	0.61
LD-96-7A Bt 2.3	0.29	1.76	0.46	0.47	2.64	0.51	100	18.26	0.61
LD-96-7G Bt 1.1	0.28	1.75	0.47	0.49	3.01	0.5	100	25.4	0.6
LD-96-7G Bt 1.2	0.28	1.76	0.47	0.48	2.89	0.5	100	15.81	0.6
LD-96-7G Bt 1.3	0.28	1.8	0.47	0.48	2.93	0.5	100	73.28	0.59
LD-96-7G Bt 2.1	0.28	1.69	0.47	0.48	3	0.49	100	14.87	0.59
LD-96-7G Bt 2.2	0.28	1.7	0.47	0.48	2.95	0.5	100	25.07	0.6

LD-96-7G Bt 2.3	0.28	1.68	0.47	0.48	2.79	0.49	29.74	14.99	0.6
LD-96-2 Bt Florettes 1.1	0.28	2.44	0.47	0.48	2.63	0.51	39.83	30.58	0.61
LD-96-2 Bt Florettes 1.2	0.29	2.24	0.44	0.47	2.8	0.55	9.13	28.72	0.68
LD-96-2 Bt Florettes 1.3	0.29	2.14	0.46	0.48	2.59	0.53	12.65	23.01	0.62
LD-96-2 Bt Florettes 1.4	0.28	2.21	0.46	0.49	2.7	0.52	14.76	28.29	0.63
LD-96-2 Bt Florettes 1.5	0.29	2.18	0.46	0.48	2.65	0.52	8.61	15.06	0.63

Mineral formulas from EPMA

Plagioclase feldspar calculated on the basis of 8 oxygens

	SiO_2	Al_2O_3	CaO	Na_2O	K_2O
Y-31 Host CP P 1.1	2.78	1.22	0.23	0.76	0.01
Y-31 Host CP P 1.2	2.76	1.24	0.24	0.75	0.01
Y-31 Host CP P 1.3	2.75	1.25	0.24	0.73	0.01
Y-31 Host CP P 2.1	2.80	1.20	0.20	0.77	0.01
Y-31 Host CP P 2.2	2.81	1.19	0.19	0.80	0.01
Y-31 Host CP P 2.3	2.81	1.18	0.19	0.80	0.01
MF-5-2 P 1.1	2.87	1.13	0.14	0.80	0.02
MF-5-2 P 1.2	2.87	1.14	0.14	0.80	0.01
MF-5-2 P 1.3	2.87	1.13	0.14	0.80	0.02
LD-96-7A P 1.1	2.84	1.16	0.15	0.79	0.02
LD-96-7A P 1.2	2.85	1.15	0.15	0.83	0.01
LD-96-7A P 1.3	2.83	1.17	0.16	0.82	0.02
LD-96-7A P 2.1	2.85	1.14	0.15	0.82	0.03
LD-96-7A P 2.2	2.85	1.15	0.15	0.81	0.02
LD-96-7A P 2.3	2.85	1.15	0.14	0.82	0.02
LD-96-7G P 1.1	3.45	0.56	0.04	0.41	0.00
LD-96-7G P 1.2	2.92	1.09	0.09	0.86	0.01
LD-96-7G P 1.3	2.89	1.12	0.11	0.85	0.01
LD-96-7G P 2.1	2.85	1.14	0.14	0.83	0.02
LD-96-7G P 2.2	2.86	1.14	0.14	0.82	0.02
LD-96-7G P 2.3	2.81	1.20	0.15	0.82	0.01
LD-96-1A P 1.1	2.98	1.05	0.04	0.85	0.00
LD-96-1A P 1.2	2.99	1.03	0.03	0.89	0.01
LD-96-1A P 1.3	2.93	1.09	0.09	0.81	0.03
LD-96-1A P 1.4	2.94	1.07	0.08	0.76	0.06
LD-96-1A P 2.1	2.97	1.06	0.03	0.67	0.21
LD-96-1A P 2.2	2.96	1.06	0.04	0.87	0.01
LD-96-1A P 2.3	2.91	1.10	0.09	0.84	0.01
LD-96-1A P 2.4	2.92	1.11	0.10	0.82	0.01
LD-96-2 P 1.1 (in Tur)	2.95	1.08	0.02	0.93	0.00
LD-96-2 P 1.1 (in Tur)	2.98	1.02	0.01	0.99	0.00
LD-96-2 P 1.1 (in Tur)	2.99	1.00	0.01	0.99	0.00
LD-96-2 P 1.1 (in Tur)	3.00	1.00	0.00	0.97	0.00
LD-96-2 P 2.1 (in Tur)	2.99	1.02	0.02	0.95	0.00
LD-96-2 P 2.1 (in Tur)	2.98	1.02	0.03	0.94	0.00
LD-96-2 P 2.1 (in Tur)	2.98	1.01	0.01	0.98	0.00

Potassium feldspar calculated on the basis of 8 oxygens

	SiO_2	Al_2O_3	Na_2O	K_2O
Y-31 Host CP K 1.1	3.00	1.01	0.07	0.91
Y-31 Host CP K 1.2	3.00	1.00	0.08	0.90
Y-31 Host CP K 1.3	3.00	1.01	0.09	0.89
Y-31 Host CP K 2.1	3.00	1.01	0.05	0.92
Y-31 Host CP K 2.2	3.00	1.01	0.05	0.93
Y-31 Host CP K 2.3	2.99	1.03	0.05	0.91
MF-1 K 1.1	3.00	1.00	0.11	0.86
MF-1 K 1.2	3.01	1.01	0.10	0.85
MF-1 K 1.3	3.01	1.00	0.11	0.84
MF-1 K 1.4	3.00	1.00	0.08	0.89
MF-1 K 2.1	3.01	1.00	0.10	0.87
MF-1 K 2.2	3.01	1.00	0.09	0.88
LD-96-7A K 1.1	3.01	0.99	0.07	0.91
LD-96-7A K 1.2	3.00	1.02	0.04	0.92
LD-96-7A K 1.3	3.00	1.02	0.04	0.91
LD-96-7A K 2.1	3.00	1.00	0.04	0.93
LD-96-7A K 2.2	3.01	0.99	0.07	0.90
LD-96-7A K 2.3	3.00	1.02	0.03	0.93
LD-96-7G K 1.1	3.00	1.00	0.07	0.89
LD-96-7G K 1.2	3.00	1.00	0.05	0.92
LD-96-7G K 1.3	3.00	1.01	0.11	0.86
LD-96-7G K 2.1	3.01	1.00	0.09	0.88
LD-96-7G K 2.2	3.00	1.00	0.08	0.89
LD-96-7G K 2.3	3.00	1.01	0.07	0.89
LD-96-1A K 1.1	2.99	1.01	0.08	0.89
LD-96-1A K 1.2	2.99	1.01	0.07	0.91
LD-96-1A K 1.3	2.99	1.02	0.06	0.93
LD-96-1A K 1.4	2.99	1.02	0.05	0.91
LD-96-1A-K 2.1	*2.72*	*1.40*	*0.10*	*0.80*
LD-96-1A-K 2.2	2.95	1.07	0.10	0.86
LD-96-1A-K 2.3	3.00	1.00	0.08	0.92

Biotite calculated on the basis of 11 oxygens

	SiO_2	TiO_2	Al_2O_3	FeO	MnO	MgO	K_2O
Y-31 Host CP Bt 1.1	2.84	0.14	1.30	1.09	0.07	1.47	0.90
Y-31 Host CP Bt 1.2	2.85	0.13	1.29	1.10	0.07	1.46	0.93
Y-31 Host CP Bt 1.3	2.86	0.11	1.31	1.05	0.07	1.54	0.88
Y-31 Host CP Bt 2.1	2.84	0.12	1.30	1.11	0.07	1.48	0.92
Y-31 Host CP Bt 2.2	2.84	0.13	1.29	1.09	0.07	1.49	0.92
Y-31 Host CP Bt 2.3	2.84	0.12	1.33	1.06	0.07	1.47	0.93
MF-1 Bt 1.1	2.88	0.16	1.25	1.00	0.07	1.54	0.89
MF-1 Bt 1.2	2.89	0.17	1.23	0.98	0.06	1.55	0.89
MF-1 Bt 1.3	2.90	0.16	1.24	0.97	0.07	1.55	0.87
MF-1 Bt 1.4	2.90	0.16	1.23	0.99	0.07	1.53	0.89
MF-1 Bt 1.5	2.89	0.16	1.25	0.99	0.06	1.54	0.86
MF-5-2 Bt 1.1	2.85	0.14	1.35	1.05	0.07	1.42	0.91
MF-5-2 Bt 1.2	2.89	0.14	1.28	1.01	0.06	1.49	0.90
MF-5-2 Bt 1.3	2.87	0.14	1.31	1.03	0.06	1.45	0.92
MF-5-2 Bt 1.4	2.87	0.16	1.28	1.04	0.07	1.46	0.92
LD-96-7A Bt 1.1	2.84	0.16	1.30	1.04	0.07	1.47	0.91
LD-96-7A Bt 1.2	2.87	0.16	1.34	0.99	0.08	1.40	0.93
LD-96-7A Bt 1.3	2.88	0.15	1.29	0.99	0.07	1.48	0.92
LD-96-7A Bt 2.1	2.87	0.13	1.29	1.03	0.07	1.50	0.91
LD-96-7A Bt 2.2	2.85	0.12	1.36	1.00	0.07	1.51	0.85
LD-96-7A Bt 2.3	2.82	0.15	1.36	1.05	0.07	1.46	0.88
LD-96-7G Bt 1.1	2.88	0.15	1.30	0.96	0.06	1.50	0.91
LD-96-7G Bt 1.2	2.86	0.15	1.30	1.01	0.06	1.50	0.90
LD-96-7G Bt 1.3	2.86	0.14	1.31	1.01	0.06	1.50	0.91
LD-96-7G Bt 2.1	2.85	0.15	1.28	1.02	0.06	1.53	0.90
LD-96-7G Bt 2.2	2.86	0.15	1.29	1.03	0.06	1.51	0.90
LD-96-7G Bt 2.3	2.85	0.15	1.30	1.01	0.06	1.51	0.87
LD-96-1A Bt 1.1	2.93	0.14	1.20	1.01	0.17	1.42	0.91
LD-96-1A Bt 1.2	2.92	0.15	1.20	0.99	0.17	1.41	0.93
LD-96-1A Bt 1.3	2.91	0.15	1.20	1.00	0.18	1.43	0.92
LD-96-1A B 2.1	2.86	0.16	1.33	0.98	0.08	1.42	0.91
LD-96-1A B 2.2	2.88	0.15	1.26	0.99	0.08	1.51	0.90
LD-96-1A B 2.3	2.90	0.16	1.26	0.99	0.08	1.47	0.91
LD-96-2 Bt Florettes 1.1	2.90	0.09	1.34	1.02	0.08	1.46	0.87
LD-96-2 Bt Florettes 1.2	2.86	0.10	1.50	1.09	0.07	1.28	0.71
LD-96-2 Bt Florettes 1.3	2.86	0.11	1.41	1.03	0.08	1.39	0.85
LD-96-2 Bt Florettes 1.4	2.91	0.10	1.39	0.98	0.07	1.41	0.84

	SiO_2	TiO_2	Al_2O_3	FeO	MnO	MgO	K_2O
LD-96-2 Bt Florettes 1.5	2.86	0.11	1.38	1.04	0.08	1.46	0.82
LD-96-2 Bt 2.1	2.84	0.09	1.44	1.06	0.08	1.45	0.77
LD-96-2 Bt 2.2	*2.86*	*0.09*	*1.43*	*1.05*	*0.08*	*1.42*	*0.82*

Minimum Detection Limits for EPMA (ppm)

Oxides	Plagioclase	K-Feldspar	Biotite
Na	150	140	150
Fe	200	210	230
Ca	120	120	140
Al	150	40	130
Mg	120	130	130
Mn	170	180	200
Ti	220	230	240
Si	170	160	160
K	90	100	110

Appendix 3

Plagioclase feldspar trace and rare earth concentrations from LA-ICP-MS

	SiO2	CaO	Sc	Ti	Mn	Zn	Ga	Ga	Rb	Sr	Y	Zr	Nb	In	Sn	Ba	La	Ce
	29	43	45	47	55	67	69	71	85	88	89	90	93	115	117	137	139	140
	wt%	wt%	ppm	ppm	ppm	ppm	ppm	ppm	ppm	ppm	ppm	ppm	ppm	ppm	ppm	ppm	ppm	ppm
Sample Name																		
Y31P1.1 55um 7Hz 58% 3.08Jcm-2	62.9	4.6	<4.31	19	<154.19	48	36	23	<2.20	772	0	0.02	0	0	<4.19	63	4.1	3.5
Y31P1.2 55um 7Hz 58% 3.20Jcm-2	62.5	3.8	<3.45	<16.58	<102.37	43	39	25	<2.30	605	0	0	0	0.03	<2.99	52	2.5	2.1
Y31P2.1 55um 7Hz 58% 2.65Jcm-2	64	<0.13	<4.19	25	<111.91	<26.39	0	<1.75	<1.77	<0.91	0	0.25	0	0.27	85	0.49	0.02	0.05
Y31P2.1 55um 7Hz 58% 2.83Jcm-2	65.9	0.21	4.2	<13.41	<88.45	<25.66	32	13	533	109	0	0	0	0	0.62	74	0.21	0.16
LD96MF5P.1 55um 7Hz 57% 3.39Jcm-2	68	1.9	19	123	<204.45	<140.19	71	33	120	252	0	18	0.39	<0.26	<14.44	146	0.96	0.86
LD96MF5P.2 55um 7Hz 57% 2.83Jcm-2	68	<0.18	13	32	<95.53	<70.37	0.11	<0.88	<0.83	<1.64	<0.37	1.1	0	<0.10	4.1	<1.15	0	<0.13
LD96-7AP1.1 55um 7Hz 58% 3.08Jcm-2	64.3	2.9	<21.78	<196.50	<269.82	<65.19	23	20	2.7	187	0	0.04	0.02	0.07	<6.30	<8.92	2.8	1.7
LD96-7AP1.2 55um 7Hz 58% 2.96Jcm-2	65.4	2.9	<12.13	<80.13	<198.86	<71.05	21	24	2.6	193	0	<1.51	0	<0.23	<5.97	<5.29	2.4	1.5
LD96-7AP1.3 55um 7Hz 58% 2.59Jcm-2	64.4	3.2	<17.80	<89.29	<334.42	<138.93	24	30	<2.90	229	0.17	0	<1.18	<0.63	<16.25	<4.27	3.1	1.9
LD96-7A P2.1 55um 7Hz 58% 2.28Jcm-2	65.2	2.4	<18.56	<137.17	<258.15	65	28	37	<6.17	243	0.04	0.12	0.04	0.07	<11.43	19	1	0.8
LD96-7A P2.2 55um 7Hz 58% 2.59Jcm-2	65.1	1.6	<25.92	<168.26	<447.37	<125.00	19	19	<1.84	160	<1.64	<1.59	0	<0.72	<15.61	<12.92	0.13	<0.81
LD96-7A P2.3 55um 7Hz 58% 2.53Jcm-2	65	2.4	<28.94	<140.59	<369.48	<109.31	41	37	<4.86	215	0	<1.39	0	<0.46	<14.71	27	0.99	1.2
LD96-7A P2.4 55um 7Hz 58% 2.77Jcm-2	65	2.5	<35.71	<215.40	<464.21	<203.17	27	24	8.2	209	0.21	0.41	0.03	<1.20	<23.42	11	3	7.9
LD96-7G P1.1 55um 7Hz 58% 2.65Jcm-2	67.6	2	<9.57	<27.71	<228.01	<48.78	19	17	<3.92	279	0.08	0	0	<0.28	<6.89	27	1.1	0.65
LD96-7G P1.2 55um 7Hz 58% 2.59Jcm-2	67.6	0.13	6	<18.39	<102.73	<35.40	21	29	586	57	0.03	0.03	0	<0.15	<7.01	21	0.17	0.15
LD96-7G P2.1 55um 7Hz 58% #.22Jcm-2	65.18	2.8	<4.93	<20.97	<139.61	<27.09	22	28	<2.91	293	0	0.04	0	0	<5.80	5.6	3.2	2.1
LD96-7G P2.2 55um 7Hz 58% 2.77Jcm-2	65.24	3	<7.90	<28.27	<217.06	<93.75	23	25	<3.95	268	0.07	0.06	0	0.04	<6.21	6.9	2.9	2.2
LD96-2P2.1 55um 7Hz 61% 3.14Jcm-2	67	0.62	7.8	<19.02	<57.58	<35.36	21	22	106	233	0.01	0.1	<0.12	<0.07	<3.69	4.3	0.01	0.025
LD96-2P2.2 55um 7Hz 61% 2.71Jcm-2	67	0.59	7.6	<9.15	<54.25	<32.08	22	28	<1.25	160	0	0.19	0.03	<0.08	<3.31	0.36	0.01	0.011

	Pr	Nd	Sm	Eu	Eu	Gd	Tb	Dy	Ho	Er	Tm	Yb	Lu	Ta	Pb	Th	U	Peak	Abltn
	141	146	147	151	153	157	159	163	165	166	169	172	175	181	208	232	238	secs	yield
	ppm	ppm	ppm	ppm	ppm	ppm	ppm	ppm	ppm	ppm	ppm	ppm	ppm	ppm	ppm	ppm	ppm		
Sample Name																			
Y31P1.1 55um 7Hz 58% 3.08Jcm-2	0.12	0.28	0	0.06	0.17	0	0	0	0	0	0	0	0	0	24	0.04	0.02	42.4	68%
Y31P1.2 55um 7Hz 58% 3.20Jcm-2	0.05	0.15	0	0.13	0.13	0	0	0	0	0	0	0	0	0	24	0	0	31.6	94%
Y31P2.1 55um 7Hz 58% 2.65Jcm-2	0	0	0	0	0	0	0	0	0	0	0	0	0	0	0.21	0.02	0.02	19.3	102%
Y31P2.1 55um 7Hz 58% 2.83Jcm-2	0.01	0	0	0.05	0.01	0	0	0	0	0	0	0	0	0	37	0.04	0.01	26.2	108%
LD96MF5P.1 55um 7Hz 57% 3.39Jcm-2	0.03	0	0	0.22	0	0	0	0	0	0	0	<1.49	0	0.13	47	6.1	2.6	7.7	68%
LD96MF5P.2 55um 7Hz 57% 2.83Jcm-2	0	0	0	0	0	0	0	0	0	0	0	0	0	0	0.9	0.01	0	12.3	119%
LD96-7AP1.1 55um 7Hz 58% 3.08Jcm-2	<1.02	0	0	0.02	0.04	<2.21	0	0	0	0	0	0	0	0	19	0.01	0.01	47	32%
LD96-7AP1.2 55um 7Hz 58% 2.96Jcm-2	0.25	0	0	0.02	0.09	0.06	<0.39	0	0	0	0	0	0	0.03	20	0	0	43.9	43%
LD96-7AP1.3 55um 7Hz 58% 2.59Jcm-2	0.03	0.2	0	0.03	0.03	0.11	0	0	0.01	0	0	0.06	0.04	0.02	21	0	0.01	41.6	26%
LD96-7A P2.1 55um 7Hz 58% 2.28Jcm-2	0.06	0	0	0.05	0.02	<6.15	0	0	0.01	0	0.02	0	0	0	27	0.01	0.03	41.6	34%
LD96-7A P2.2 55um 7Hz 58% 2.59Jcm-2	<1.10	0	0	<1.00	0.12	0	0	0	0	0	0	0	0	<0.48	19	0.02	0.01	43.2	20%
LD96-7A P2.3 55um 7Hz 58% 2.53Jcm-2	0.04	0	<3.02	0	0.04	0	0	0	0	0	0	0	0	0	28	0	0.01	36.2	24%
LD96-7A P2.4 55um 7Hz 58% 2.77Jcm-2	0.19	0	0	0.04	0.2	0	<0.46	0	<0.94	0	<0.43	0	0	0	22	0.05	0.6	43.9	19%
LD96-7G P1.1 55um 7Hz 58% 2.65Jcm-2	0.04	0.23	0	0.13	0.02	0	0	0	<0.91	0	0	0	0	<0.23	23	0	0.29	33.9	38%
LD96-7G P1.2 55um 7Hz 58% 2.59Jcm-2	0	0.05	0	0	0	0	0	0	0	0	0	0	0	0.01	41	0	0.06	23.9	84%
LD96-7G P2.1 55um 7Hz 58% #.22Jcm-2	0.07	0.19	0	0.08	0.11	0	0	0	0	0	0	0	0	0	20	0	0.09	49.3	55%
LD96-7G P2.2 55um 7Hz 58% 2.77Jcm-2	0.06	0	0	0	0	0	0	0	0	0	0	0	0	0	18	0.01	0.41	42.4	38%
LD96-2P2.1 55um 7Hz 61% 3.14Jcm-2	0	0	0	0.005	0.004	0.02	0	0	0	0	0	0	0	0.01	18	0.05	0.03	48.6	64%
LD96-2P2.2 55um 7Hz 61% 2.71Jcm-2	0.002	0	0	0	0	0	0	0	0	0	0	0	0	0	7.3	0.05	0.04	45.5	78%

Potassium feldspar trace and rare earth concentrations from LA-ICP-MS

	SiO2	CaO	Sc	Ti	Mn	Zn	Ga	Ga	Rb	Sr	Y	Zr	Nb	In	Sn	Ba	La	Ce
	29	43	45	47	55	67	69	71	85	88	89	90	93	115	117	137	139	140
	wt%	wt%	ppm	ppm	ppm	ppm	ppm	ppm	ppm	ppm	ppm	ppm	ppm	ppm	ppm	ppm	ppm	ppm
Sample Name																		
Y31K1.1 55um 7Hz 58% 2.96Jcm-2	65.5	0.39	<3.77	25	<97.48	267	270	19	539	242	0.05	0	0	0.01	<3.65	879	0.3	0.71
Y31K1.2 55um 7Hz 58% 3.51Jcm-2	65.2	0.52	<3.99	27	<95.86	128	145	11	571	296	0	0.04	0.01	0	<4.65	468	0.25	0.09
LD96-7A K2.1 55um 7Hz 58% 2.40Jcm-2	65.6	<0.27	<6.27	<45.18	<96.49	22	24	23	780	94	<0.36	<0.35	0	<0.23	<3.95	49	0.34	<0.26
LD96-7A K2.2 55um 7Hz 58% 2.34Jcm-2	65.8	<0.42	<10.22	<63.56	<132.03	82	98	22	599	116	0.17	0	0.01	0.01	<11.49	358	0.17	0.03
LD96-7A K2.3 55um 7Hz 58% 2.16Jcm-2	65.4	<0.54	<18.88	<83.30	<233.50	<77.16	31	23	625	164	<2.55	0	<0.40	<0.38	<10.18	53	0.23	0.13
LD96-7G K1.1 55um 7Hz 58% 3.02Jcm-2	65.62	0.12	3.9	13	<58.21	185	177	16	664	69	0	0.26	0	<0.25	<6.01	619	0.21	0.2
LD96-7G K2.1 55um 7Hz 58% 2.71Jcm-2	65.46	<0.27	<6.29	<29.64	<154.72	<50.89	28	16	526	187	0	0.05	0	0.05	<7.26	60	0.37	0.11

	Pr	Nd	Sm	Eu	Eu	Gd	Tb	Dy	Ho	Er	Tm	Yb	Lu	Ta	Pb	Th	U		Peak	Abltn
	141	146	147	151	153	157	159	163	165	166	169	172	175	181	208	232	238		secs	yield
	ppm	ppm	ppm	ppm	ppm	ppm	ppm	ppm	ppm	ppm	ppm	ppm	ppm	ppm	ppm	ppm	ppm			
Sample Name																				
Y31K1.1 55um 7Hz 58% 2.96Jcm-2	0.01	0.03	<0.90	0.06	0.14	0	0	0	0	0	0	0	0	0.04	50	0.01	0.03		38.6	90%
Y31K1.2 55um 7Hz 58% 3.51Jcm-2	0	0	0	0.14	0.06	0.08	0	0	0	0	0	0	0	0.03	70	0	0		47.8	96%
LD96-7A K2.1 55um 7Hz 58% 2.40Jcm-2	<0.15	0	0	0.02	0.04	0	0	0	0	0	0	0	0	0.01	167	0.12	0.12		12.3	115%
LD96-7A K2.2 55um 7Hz 58% 2.34Jcm-2	0	0	0	0.03	0	0	0.01	0	0	0	0	0	0	0.04	61	0	0.01		33.2	64%
LD96-7A K2.3 55um 7Hz 58% 2.16Jcm-2	<0.26	0.09	<3.59	0	0.14	0	0	0	<0.21	0	0	0	0	0	73	0	0		33.2	35%
LD96-7G K1.1 55um 7Hz 58% 3.02Jcm-2	0	0	0	0.02	0	0	0	<0.26	0	0	0	0	0	0.08	68	0.06	0.41		17.7	162%
LD96-7G K2.1 55um 7Hz 58% 2.71Jcm-2	0	0	0	0	0.02	0	0	0	0	0	0	0	0	0.02	50	0	0.03		42.4	46%

Biotite trace and rare earth concentrations from LA-ICP-MS

	SiO2	CaO	Sc	Ti	Mn	Zn	Ga	Ga	Rb	Sr	Y	Zr	Nb	In	Sn	Ba	La	Ce
	29	43	45	47	55	67	69	71	85	88	89	90	93	115	117	137	139	140
	wt%	wt%	ppm	ppm	ppm	ppm	ppm	ppm	ppm	ppm	ppm	ppm	ppm	ppm	ppm	ppm	ppm	ppm
Sample Name																		
Y31B1.1 55um 7Hz 58% 2.59Jcm-2	37.78	0.04	38	13410	7639	1558	487	47	781	1.4	0.1	0.08	11	0.51	1.8	1490	0.13	0.11
Y31B1.2 55um 7Hz 58% 2.46Jcm-2	37.87	0.03	37	12918	7400	1166	76	46	1282	0.86	0	0.05	10	0.49	<1.54	134	0.14	0.15
Y31B1.3 55um 7Hz 58% 2.96Jcm-2	38.23	0.04	43	14779	7940	1498	360	51	764	1.3	0.06	0.12	12	0.47	1.8	1123	0.23	0.22
Y31B2.1 55um 7Hz 58% 3.27Jcm-2	37.96	0.03	49	12920	7865	1543	426	53	837	1.3	0.01	0.16	13	0.59	1.9	1352	0.23	0.14
Y31B2.2 55um 7Hz 58% 2.71Jcm-2	37.88	0.05	48	11620	8100	1951	717	58	630	1.2	0.06	0.33	7.6	0.55	1.8	2327	1	0.68
Y31B2.3 55um 7Hz 58% 2.96Jcm-2	37.9	0.04	54	11953	7814	1610	551	51	563	1.8	0.07	0.08	9.3	0.57	1.8	1763	0.37	0.27
LD96M1.1 55um 7Hz 57% 3.45Jcm-2	38	0.09	46	18308	7618	1032	39	44	1104	0.35	0.005	2.9	27	0.39	4.7	6.9	0.13	0.11
LD96M1.2 55um 7Hz 57% 3.33Jcm-2	38	0.09	46	17813	7711	1008	40	44	1027	0.37	0.01	2.9	26	0.41	4.7	6.9	0.16	0.13
LD96M1.3 55um 7Hz 57% 3.20Jcm-2	38	0.08	46	17881	7896	1008	39	44	1142	0.43	0.01	2.9	28	0.38	4.8	6	0.11	0.1
LD96M1.4 55um 7Hz 57% 3.14Jcm-2	38	0.1	51	18154	8587	1041	42	45	994	0.49	0.01	5.2	29	0.47	5.3	14	0.08	0.07
LD96MF5.1 55um 7Hz 57% 3.20Jcm-2	38	0.13	47	15039	9286	1611	411	54	1131	0.75	0.1	0.35	12	0.38	2.3	1823	0.05	0.04
LD96MF5.2 55um 7Hz 57% 3.08Jcm-2	38	1.9	46	16034	8933	1483	332	52	916	9.4	1.3	0.11	11	0.43	2.5	1559	30	38
LD96MF5.3 55um 7Hz 57% 2.83Jcm-2	38	0.12	41	14088	8172	1465	384	48	792	0.78	0.08	0.37	11	0.38	3.1	1756	0.39	0.37
LD96-7ABt1.1 55um 7Hz 58% 3.02Jcm-2	37.9	0.09	67	17125	9134	1707	587	55	546	1	0.1	0.1	23	0.48	3.5	2253	0.58	0.67
LD96-7ABt1.2 55um 7Hz 58% 3.02Jcm-2	38.3	0.06	67	17086	8255	1631	534	52	666	0.66	0.06	0.09	20	0.51	2.9	1925	0.39	0.3
LD96-7ABt1.3 55um 7Hz 58% 3.14Jcm-2	38.7	0.08	69	15213	8713	1620	439	57	629	1.3	0.13	0.63	20	0.58	3.4	1546	2.9	2.8
LD96-7ABt1.4 55um 7Hz 58% 2.83Jcm-2	38.7	<0.08	69	17402	8546	1593	464	54	715	0.85	0.16	0.09	19	0.54	2.4	1620	1.7	1.5
LD96-7ABt2.1 55um 7Hz 58% 2.90Jcm-2	38.5	0.16	62	15621	8732	1691	425	57	1019	1.4	0.35	0.04	16	0.55	2.6	1435	4	6.7
LD96-7ABt2.2 55um 7Hz 58% 2.65Jcm-2	38.3	0.08	64	14987	8713	1399	177	59	769	4.8	0.23	0.12	18	0.51	3	501	3.4	3.2
LD96-7G B1.1 55um 7Hz 58% 2.53Jcm-2	38.27	0.07	70	16770	7410	1330	443	48	688	0.89	0.06	0.19	24	0.33	4.78	1533	0.51	0.27
LD96-7G B1.2 55um 7Hz 58% 3.51Jcm-2	38.05	0.12	66	15497	7213	1213	385	45	879	1.1	0.18	0.1	22	0.33	4.07	1441	2	2.4
LD96-7G B1.3 55um 7Hz 58% 2.28Jcm-2	38.18	0.05	68	17250	7563	1494	660	43	935	0.58	0.08	0.09	23	0.35	3.63	2447	0.31	0.23
LD96-7G B2.1 55um 7Hz 58% 2.40Jcm-2	38.35	0.078	47	17011	7588	1278	308	55	1023	1.3	0.92	0.17	23	0.37	4.7	979	7.4	11
LD96-7G B2.2 55um 7Hz 58% 2.22Jcm-2	38.22	<0.05	44	16173	8105	1298	315	49	1172	0.69	0.1	0.13	23	0.26	4	1036	1.1	1.5
LD96-2BF1 55um 7Hz 61% 2.83Jcm-2	38	0.12	310	10845	8849	1561	63	73	1566	2.2	0.19	1.3	23	0.88	35	9.4	1.5	1.8
LD96-2BF2 55um 7Hz 61% 3.08Jcm-2	38	0.11	300	10672	8809	1644	68	75	1662	2.8	0.12	1	19	0.87	30	34	1.6	1.7
LD96-2BF3 55um 7Hz 61% 2.90Jcm-2	38	0.26	203	7337	8774	1998	130	147	972	7.5	0.54	6.5	35	1	24	25	15	16
LD96-2BF4 55um 7Hz 61% 3.08Jcm-2	38	0.27	64	891	12622	3068	179	216	54	4.5	0.43	12	6.3	1.2	4.2	6.1	10	11

	Pr	Nd	Sm	Eu	Eu	Gd	Tb	Dy	Ho	Er	Tm	Yb	Lu	Ta	Pb	Th	U		Peak	Abltn
	141	146	147	151	153	157	159	163	165	166	169	172	175	181	208	232	238		secs	yield
	ppm	ppm	ppm	ppm	ppm	ppm	ppm	ppm	ppm	ppm	ppm	ppm	ppm	ppm	ppm	ppm	ppm			
Sample Name																				
Y31B1.1 55um 7Hz 58% 2.59Jcm-2	0.01	0.05	0	0.04	0.05	0	0	0	0	0	0	0	0	0.18	2.5	0.01	0.07		47	254%
Y31B1.2 55um 7Hz 58% 2.46Jcm-2	0.01	0.05	0	0	0.02	0	0	0	0	0	0	0	0	0.12	1.8	0.005	0.03		47	253%
Y31B1.3 55um 7Hz 58% 2.96Jcm-2	0.02	0.02	0	0.01	0.05	0.02	0	0	0	0	0	0	0	0.2	2.3	0.01	0.03		47	306%
Y31B2.1 55um 7Hz 58% 3.27Jcm-2	0.01	0.02	0	0.003	0.01	0.02	0	0	0	0	0	0	0	0.17	2.2	0.05	0.05		49.3	308%
Y31B2.2 55um 7Hz 58% 2.71Jcm-2	0.05	0.06	0	0.02	0.03	0.03	0	0	0	0	0	0	0	0.14	3.2	0.27	0.25		44.7	300%
Y31B2.3 55um 7Hz 58% 2.96Jcm-2	0.03	0.04	0	0.03	0.01	0.01	<0.03	0	0	0	0	0	0	0.08	2.2	0.09	0.04		48.6	293%
LD96M1.1 55um 7Hz 57% 3.45Jcm-2	0.008	0.018	0	0.001	0	0.01	0.001	0	0	0	0	0.002	0.001	0.35	1.7	0.014	0.006		49.3	322%
LD96M1.2 55um 7Hz 57% 3.33Jcm-2	<0.04	0.007	0.004	0	0.002	<0.13	0	0	0	0	0	0	0.001	0.38	1.6	0.01	0.011		50.1	317%
LD96M1.3 55um 7Hz 57% 3.20Jcm-2	0.009	0.015	0	0	0	0	0.001	0	0	<0.05	0	0	0.001	0.39	1.6	0.006	0.006		49.3	302%
LD96M1.4 55um 7Hz 57% 3.14Jcm-2	0.006	0.007	0	0	0.002	0	0	0	0	0	0	0.005	0.001	0.38	1.6	0.013	0.009		49.3	314%
LD96MF5.1 55um 7Hz 57% 3.20Jcm-2	0.002	0.01	0	0.25	0.31	0.03	0.001	0	0	0	0	0	0.001	0.21	1.6	0	0.03		48.6	442%
LD96MF5.2 55um 7Hz 57% 3.08Jcm-2	2.6	6.7	0.86	0.43	0.51	0.74	0.04	0.19	0.03	0.14	0.02	0.13	0.032	0.17	2.2	1.6	1.2		45.5	392%
LD96MF5.3 55um 7Hz 57% 2.83Jcm-2	0.02	0.03	0.01	0.25	0.36	0.05	0	0.01	0	0	0.001	0	0.001	0.18	2.7	0.01	0.51		48.6	454%
LD96-7ABt1.1 55um 7Hz 58% 3.02Jcm-2	0.07	0.11	0.01	0.07	0.19	<0.39	0.003	0.01	0.001	0.01	0.002	0	0.001	0.29	2.3	0.01	0.01		49.3	365%
LD96-7ABt1.2 55um 7Hz 58% 3.02Jcm-2	0.02	0.06	0.03	0.06	0.08	0.06	0.001	0	0.002	0.003	0.001	0.01	0.001	0.19	1.8	0.005	0.01		50.1	346%
LD96-7ABt1.3 55um 7Hz 58% 3.14Jcm-2	0.24	0.59	0.07	0.08	0.12	0.09	0.002	0.01	0.01	0.01	0	0.03	0.003	0.27	2.2	0.003	0.32		50.1	341%
LD96-7ABt1.4 55um 7Hz 58% 2.83Jcm-2	0.12	0.26	0.02	<0.07	0.1	0.04	0	0.004	0	0.003	0.001	0.01	0.004	0.21	2.2	0.001	0.03		50.9	321%
LD96-7ABt2.1 55um 7Hz 58% 2.90Jcm-2	0.38	1.1	0.19	0.08	0.13	0.08	0.01	0.03	0.01	<0.08	0.001	0.04	0.005	0.22	2.4	0.14	0.92		50.9	323%
LD96-7ABt2.2 55um 7Hz 58% 2.65Jcm-2	0.22	0.63	0.05	0.03	0.02	0.05	0.003	0.02	0.01	0.01	0.01	0.004	0.002	0.2	2.3	0.01	0.16		50.1	315%
LD96-7G B1.1 55um 7Hz 58% 2.53Jcm-2	0.03	0.05	0.01	0.03	0.06	0.03	0	0	<0.05	0.01	0	0	0.001	0.3	2.2	0.02	0.02		47.8	307%
LD96-7G B1.2 55um 7Hz 58% 3.51Jcm-2	0.21	0.62	0.06	<0.06	0.09	0.05	0.004	0.03	<0.02	0.01	0.005	0.01	0.001	0.27	1.9	0.05	0.07		47.8	329%
LD96-7G B1.3 55um 7Hz 58% 2.28Jcm-2	0.01	0.05	0.01	0.06	0.08	<0.40	0.002	0	0	0	0	0.03	0.001	0.29	2.3	0.03	0.03		45.5	290%
LD96-7G B2.1 55um 7Hz 58% 2.40Jcm-2	0.94	3.2	0.37	0.09	0.12	0.32	0.03	0.13	0.03	0.07	0.01	0.06	0.01	0.35	4.1	0.01	0.14		45.5	277%
LD96-7G B2.2 55um 7Hz 58% 2.22Jcm-2	0.1	0.23	0	0.04	0.09	0	0	0.04	0.01	0.01	0	0.01	0	0.33	2.6	0.02	0.07		10	367%
LD96-2BF1 55um 7Hz 61% 2.83Jcm-2	0.09	0.29	0.05	0.005	0.01	0.03	0.01	0.01	0.003	0.02	<0.02	0.005	<0.02	1.7	6.1	0.95	1.3		48.6	247%
LD96-2BF2 55um 7Hz 61% 3.08Jcm-2	0.12	0.2	0.06	<0.03	0.01	0.05	0.001	0.01	0.004	0.013	0.001	0.004	0.002	0.82	5.9	1.2	1.2		47	260%
LD96-2BF3 55um 7Hz 61% 2.90Jcm-2	0.85	2.1	0.25	0.03	0.04	0.17	0.01	0.05	0.011	0.037	0.01	0.03	0.01	1.5	19	2	2.7		47	213%
LD96-2BF4 55um 7Hz 61% 3.08Jcm-2	0.65	1.4	0.14	0.02	0.02	<0.30	0.01	0.03	0.015	0.027	0.01	0.05	0.01	0.5	19	5.2	4		47	210%

Appendix 4

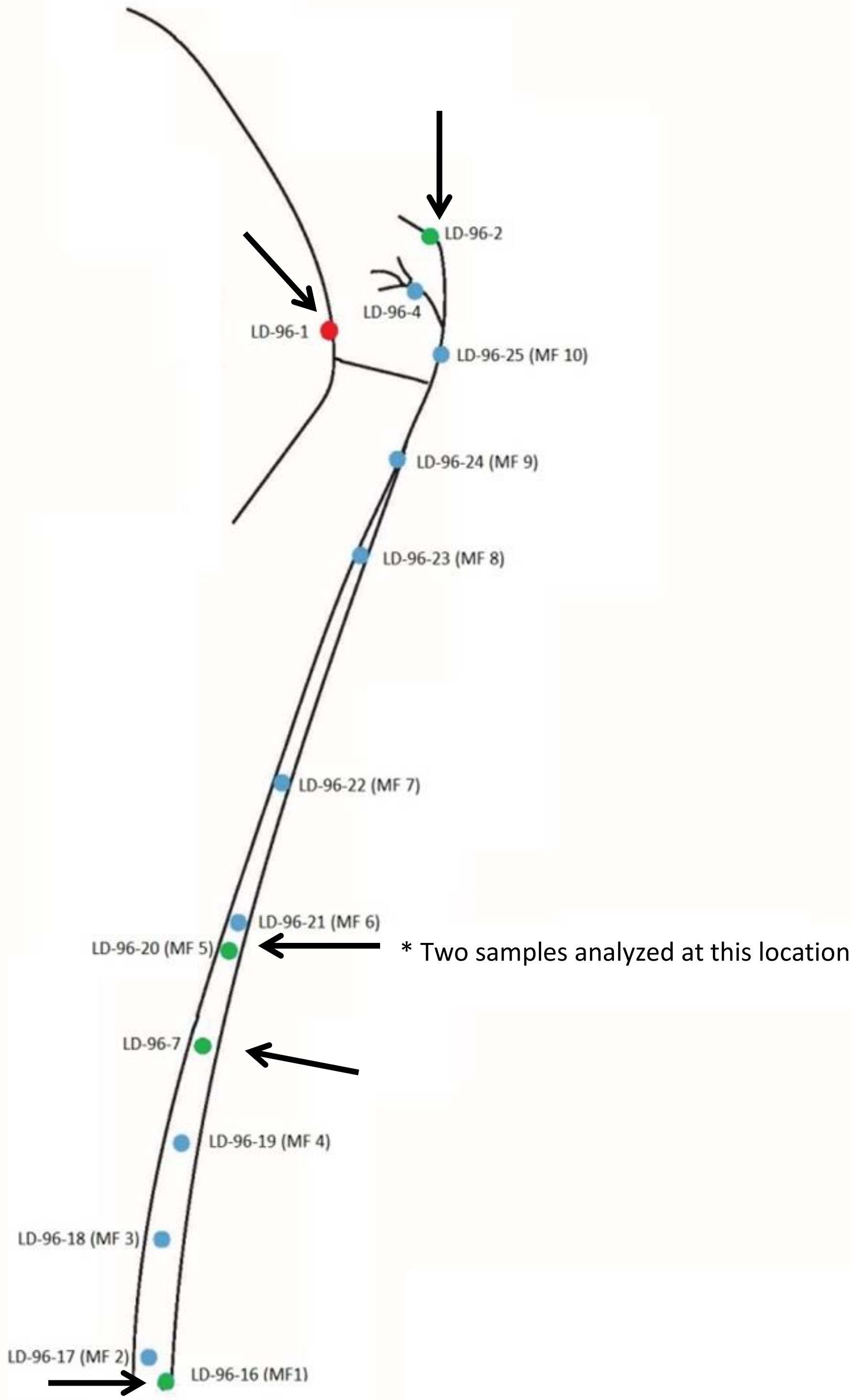

Schematic diagram showing the locations of the samples on the dike; the dike is drawn in the fine line and the country rock is outlined in the bold line.

Appendix 5

Rare earth and trace element concentrations from LA-ICP-MS in biotite

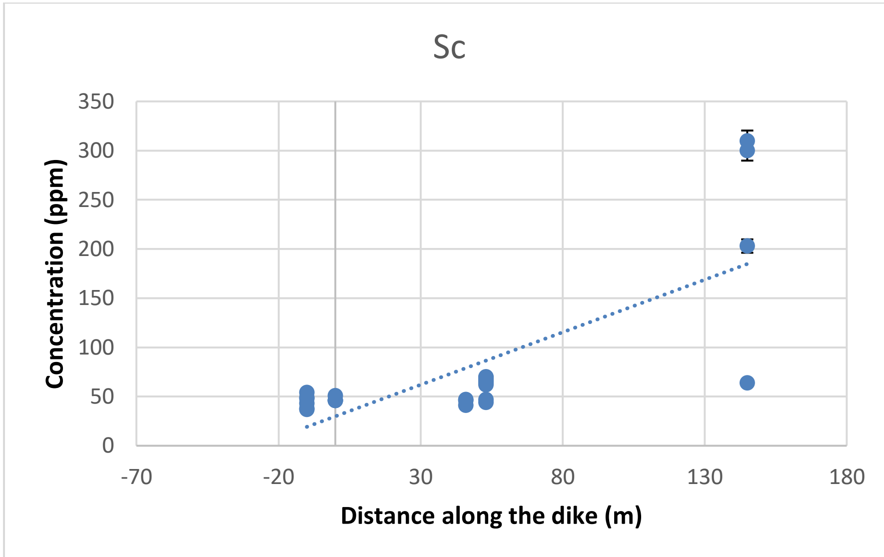

Scandium concentration

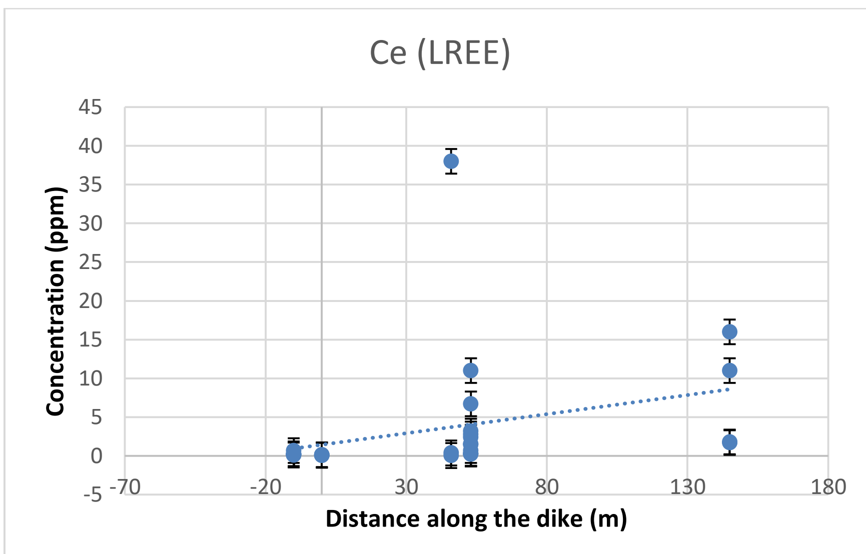

Cesium concentration (representative of other light rare earth elements)

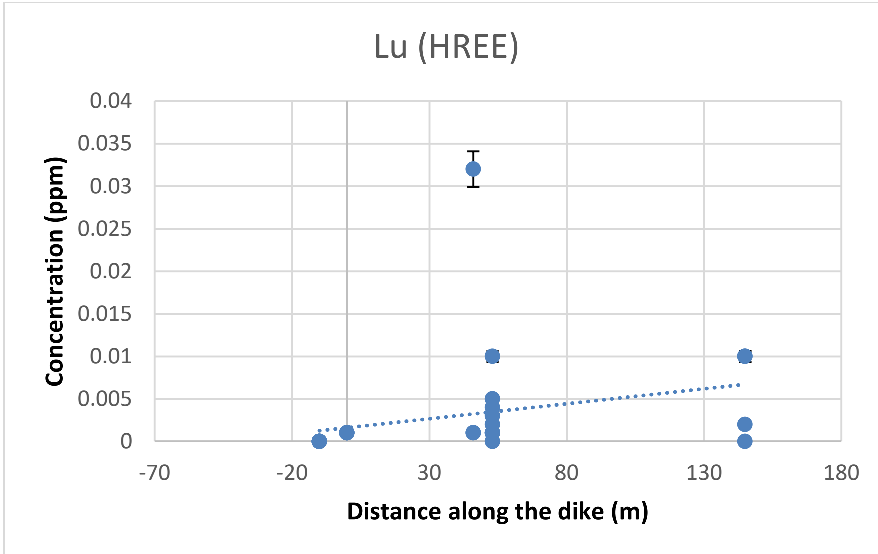

Lutetium concentration (representative of other heavy rare earth elements)

Appendix 6

Honor Code

I pledge on my honor that I have not given or received any unauthorized assistance on this assignment or examination.

Rhobeca Oliveros

November 21, 2017